

RELAXATION AND CROSS RELAXATION: NMR DETERMINATIONS OF
WATER INTERACTIONS WITH PROTEINS

Thomas F. Kumosinski and Helmut Pessen

TABLE OF CONTENTS

I.	Introduction	220
II.	Theory	221
	A. General Nonideal Effects	221
	B. Derivation of Requisite Expressions	223
	C. Evaluation of Data	226
III.	Relaxation: ^2H NMR	227
	A. Influence of Protein Hydrophilic Self-Association: β -Lactoglobulin A	227
	1. Experimental Procedures	228
	a. Preparation of Solutions	228
	b. Relaxation Measurements	228
	2. Analysis of Data	230
	a. Activities and the Multicomponent Expression	230
	b. Isotropic Binding, Two-State Model	231
	i. Determination of Correlation Times	231
	ii. Determination of Hydration Parameters	233
	iii. Comparison of Results with Other Structural Information	236
	c. Contrast of NMR Hydration with Preferential Hydration	237
	i. Isotropic Binding, Three-State Model	238
	ii. Anisotropic Binding Mechanism	240
	B. Influence of Protein Hydrophobic and Electrostatic Self-Association: Bovine Casein	240
	1. Experimental Procedures	241
	a. Preparation of Solutions	241
	b. Relaxation Measurements	241
	2. Analysis of Data	241
	a. General Considerations	241
	b. Hydration and Dynamics: Isotropic Model	242
	c. Derived Molecular Parameters of the Protein	244
	d. Hydration: Anisotropic Tumbling Model	246
IV.	Cross Relaxation	247
	A. Influence of Environmental Changes on β -Lactoglobulins	247
	1. Experimental Procedures	247
	a. Preparation of Solutions	247
	b. Relaxation Measurements	247
	2. Analysis of Data	248
	a. Relaxation Increments and Free-Water Relaxation Rates	248
	b. Structural States and Hydration	248
	c. Dynamics and Hydration from Transverse Relaxation	251

d.	Cross Relaxation and Longitudinal Relaxation	252
e.	Significance of Parameters	254
3.	Appendix	255
a.	Parameters from Transverse Relaxation Increments and Solvent Relaxation Rates	255
b.	Cross-Relaxation Increment	255
c.	Parameters from Longitudinal Relaxation Increments and Solvation Relaxation Rates	256
B.	Overview	257
V.	Concluding Remarks	257
	Acknowledgment	258
	References	259

I. INTRODUCTION

The importance of water interactions with naturally occurring biological macromolecules to the scientific community is well documented.¹ It is thought that the quantitation of this interaction will go a long way toward enabling investigators to understand the energetics of protein secondary, tertiary, and quaternary structure as well as changes in the relevant structural parameters with varying environmental conditions. However, to date not even the amount of water bound to a globular protein (hydration) can be determined with confidence, much less can one directly observe the constituent groups on the protein responsible for the binding of water. Only the concept of hydrophobic and hydrophilic interaction, as quantitated by solubilities of the individual amino acids, allows some qualitative extrapolation to the macromolecular system. To complicate the problem further, the hydration of a protein has been found to be dependent on the methodology used in the study. Traditionally, the hydrodynamic methods, i.e., sedimentation, translational and rotational diffusion, and viscosity, have been used to measure the hydration of proteins, with some success; with these, however, unlike with small angle X-ray scattering (SAXS), an assumption of the overall shape of the unhydrated protein must be made.

Recently it has been shown that, in investigating hydration, the hydrodynamic approach cannot stand alone.^{2,3} At best, it requires supplementation by a structural method, preferably SAXS, to give unequivocal information on hydration. It has also been demonstrated that sedimentation and SAXS information can be correlated to such an extent that sedimentation parameters are fairly predictable and, in effect, do not constitute an independent method. It would appear, then, that for the purpose of investigating hydration, SAXS could be considered a more useful approach than sedimentation, and that it might replace the latter, were it not for the circumstance that, in contemporary laboratories, SAXS instruments are even rarer than analytical ultracentrifuges.

As a practical matter, the SAXS method suffers from the lack of a substantial published data base. It would of course be helpful if investigators reporting SAXS results on a protein in each instance undertook the routine labor of calculating and reporting a full set of the parameters their data are capable of generating⁴ instead of merely those engaging their immediate attention. Further, it is to be hoped that those interested in hydration and structural information obtain access in larger numbers to instrumentation enabling them to use this powerful and versatile

method which, with the commercial availability in recent years of position-sensitive detectors, has been a very productive method as well.

In lieu of SAXS data, it will be shown in this chapter that NMR is capable of giving information on hydration. While the absolute values of NMR hydration are not completely independent of assumptions regarding mechanism, relative values are largely independent of such assumptions and can serve to assess changes in structure or biochemical behavior as a function of varying environmental conditions. The interpretation of such changes of course will depend on the system studied.

One way of using NMR relaxation to obtain this kind of information has been by means of frequency dependence.⁵ There are, however, few instruments available that allow dispersive measurements. Attention must also be paid to the frequencies chosen: if measurements are made at two different frequencies to eliminate one of the modes of relaxation employed here (see Equations 16a and b), care must be taken that the frequencies are sufficiently different to exhibit a substantial enough dispersion for adequate relaxation statistics. In any case, the frequencies must be high enough (and so must the molecular weight, on which the correlation time depends) to escape the line-narrowing region, i.e., the product $\omega_0^2 \tau_c^2$ (where ω_0 is the Larmor frequency and τ_c the correlation time) must be clearly larger than 1. Otherwise, the system of requisite simultaneous equations will either have no solution, or the solution will be very imprecise.

In place of frequency dependence, concentration dependence (readily accessible with any NMR instrument) may be emphasized to advantage. Two modes of relaxation, spin-lattice and spin-spin, have been used with deuteron resonance to avoid the cross relaxation encountered with spin-lattice relaxation of protons. ¹⁷O relaxation has also been used, for similar reasons.^{6,7} In a different method, proton spin-lattice relaxation has been employed, but cross-relaxation effects were determined and allowed for by the joint examination of two genetic variants of the same protein, which differed only in the known extent of an association reaction.⁸ Again, the combination of protein molecular weight and resonant frequency must satisfy the condition for avoiding the line-narrowing mentioned.

In addition to hydration, NMR relaxation can give other valuable information that can be correlated with structural and biochemical changes. Correlation times are related to molecular size and shape and are relevant to hydrodynamics. Virial coefficients, for which concentration dependence data are indispensable, can be evaluated directly from a concentration plot. It is true for either mode of relaxation that the observed relaxation rates are linear functions of hydration, concentration, and an exponential containing both the concentration and the virial coefficient B_0 . It can be seen that nonlinear regression applied to this relationship will give B_0 directly. Virial coefficients, related to the average net charge carried by molecules, provide a particularly useful measure of molecular interaction.

II. THEORY

A. General Nonideal Effects

Proteins, by their very nature as polyelectrolytes with large charge-to-mass ratios, are susceptible to severe interaction effects in solution. Although the consequent deviations from ideality are among the most important effects in solution theory, they have not received sufficient consideration in NMR studies of proteins. A prime example is the nonideality caused by repulsion due to net positive or negative charges, which has been demonstrated to have serious effects on measurements other than NMR (light scattering, osmotic pressure, sedimentation equilibrium and velocity, translational diffusion, and even pH titration⁹⁻¹³). Thus Pedersen,¹¹ on the basis of the theory of Tiselius,¹² as early as 1940 showed that high net charges on a macromolecule result in the creation of a potential gradient in a sedimenting solution during both equilibrium and velocity runs; Booth¹³ has quantitated this behavior by a general theory for charged spheres. Sedimentation coefficients of bovine serum albumin at acid pH are lower by

at least half when compared with the same protein in the presence of 0.1 M salt;¹⁴ the salt thus minimizes the high repulsive effect of the molecular charges. Light scattering and osmotic pressure measurements of aqueous proteins carrying high net charge indicate decreased apparent weight-average molecular weights with increasing concentration, in consequence of intermolecular repulsion,^{9,15-17} according to the equation:

$$M_{w,app}^{-1} = M_{w,o}^{-1} (1 + c \ln \gamma/dc) \quad (1)$$

where γ is the activity coefficient of the protein at a concentration c , $M_{w,app}$ is the experimentally derived apparent weight-average molecular weight, and $M_{w,o}$ is the true molecular weight at infinite dilution of the protein. From the virial expansion for osmotic pressure follows

$$\ln \gamma/dc = 2B_0 + 3B c + \dots \quad (2)$$

where the B quantities are the second and higher virial coefficients; for a repulsive effect usually $\ln \gamma/dc = 2 B_0 > 0$ (i.e., $\gamma > 1$), in accord with general electrolyte solution theory.

Beyond simple electrostatic repulsion, one needs to be concerned with a less obvious phenomenon, namely the charge fluctuations treated in the theory of Kirkwood and Shumaker.¹⁸ Extensive experimental evidence for this theory has been furnished by many investigations using light scattering: for proteins in water under isoionic conditions, the apparent weight-average molecular weight increases with increasing concentration.¹⁹⁻²² Ordinarily, this phenomenon might be interpreted simply as an aggregation of the molecule. However, Kirkwood and Shumaker have shown that, since proteins are polyampholytes rather than simple polyelectrolytes, attractive forces arise in isoionic protein solutions from statistical fluctuations, both in charge and in charge distribution; these in turn are associated with fluctuations in the number and configurations of protons bound to the protein molecule. Briefly stated, one or more virial coefficients in $c^{n/2}$ powers must be added to Equation 2, and these coefficients, due to progressive ionization of the macromolecule, have negative values. Moreover, the virial coefficients of the c^n terms should also usually be negative. Experimental results show the virtual elimination of such charge-fluctuation effects in the presence of a moderate amount of salt. Since virial effects are found for other solution parameters, such as sedimentation coefficients, intrinsic viscosities, and linear as well as rotational diffusion coefficients, charge fluctuations can be expected to affect these hydrodynamic parameters also.

Specifically, the translational diffusion coefficient D_t and the rotational diffusion coefficient D_r exhibit the influence of the activity coefficient, γ , which expresses the combined result of all such effects, according to

$$D_t = (8/6)D_r = [kT/(6\pi\eta r_s)](1 + c \ln \gamma/dc) \quad (3)$$

where k is Boltzmann's constant, 1.3806×10^{-16} erg $^{\circ}\text{K}^{-1}$, T is the temperature in K, η is the viscosity of the solvent, and r_s is the Stokes radius of the macromolecule. Accordingly, electrostatic repulsion and charge fluctuation will affect these, as well as other hydrodynamic parameters.

Measurements of protein hydration by NMR relaxation techniques using the two-state model of Zimmerman and Brittin²³ have yielded surprisingly large values for the correlation time of bound water when cross-relaxation effects were avoided by experiments in D_2O .^{6,24} When cross-relaxation effects were not taken into account (e.g., in proton NMR of water), correlation times obtained from dispersion data also were high,^{5,6,24,25} even though Andree²⁶ had shown that apparent τ_c values from frequency dependence of spin-lattice relaxation should be smaller as a result of cross-relaxation. Also, recent ^{17}O NMR T_1 and T_2 data of Halle et al.,⁷ give τ_c values larger than would be predicted by the Debye-Stokes-Einstein equation, a result attributed by the authors to long-range coulombic protein-protein interactions. However, these measurements as

well as many others were made, again, on isoionic protein solutions with no added salt. However, since rotational diffusion is basic to these measurements (i.e., the bound water rotates with substantially the same τ_c as the protein) and is related to τ_c (i.e., $\tau_c = r^2/6D_r$), it can be seen from Equation 3 that

$$\tau_c = [4\pi\eta r^2/(3kT)](1 + c \ln \gamma/dc)^{-1} \quad (4)$$

and, therefore, not only electrostatic effects due to the high charge-to-mass ratio of the protein but also charge-fluctuation effects should be encountered, both as a result of the methodology of these measurements. The absence of salt and the consequently large negative virial coefficients thus account for the excessive apparent τ_c values observed. The addition of salt should then result in correlation times more in accord with those calculated for the protein from structural considerations directly. In fact, two recent studies,^{8,27} using different means to deal with the complicating effects of cross-relaxation, but both using salt, obtained τ_c values in good agreement with the known structure.

B. Derivation of Requisite Expressions

In order to address this problem, one clearly should work with solutions containing salt. The theory now needs to be expanded to accommodate a three-component system. Expressions for NMR relaxation rates are rederived here in terms of the multicomponent theory of Casassa and Eisenberg,²⁸ since the salt components can compete with water for binding sites on the protein molecule (e.g., charged side chains).

The model used as a point of departure for this derivation is a fast-exchange, two-state, three-component system. The initial assumptions are (1) only one correlation time exists for the bound-water state; (2) there is competition between bound water and salt for the interaction sites on the surface of the protein; but (3) there is no competition between salt and protein for water (since experiments were performed here only on protein solutions with added salt, not on insoluble or powdered samples). Hence, a general equilibrium expression for the binding is



where P, W, and X represent protein, water, and salt at free concentrations p, w, and x, bound concentrations p_b , w_b , and x_b , and total concentrations

$$P = p + p_b \quad (5a)$$

$$W = w + w_b \quad (5b)$$

$$\text{and } X = x + x_b \quad (5c)$$

respectively. Associated with the formation of each species PW_iX_j is an apparent macroscopic association constant K_{ij} . Then

$$p_b = p \sum_{i=0}^q \sum_{j=0}^r K_{ij} w^i x^j \quad (6a)$$

where q and r are any positive integers such that $q + r = n$, the total number of binding sites per molecule. At the same time,

$$w_b = p \sum \sum_i K_{ij} w^i x^j \quad (6b)$$

$$\text{and } x_b = p \sum \sum_j K_{ij} w^i x^j \quad (6c)$$

The average number of molecules of water or salt bound to a molecule of protein, i.e., the Scatchard hydration, \bar{v}_w , and salt binding \bar{v}_x , respectively, are then given by

$$\bar{v}_w = w_b/P \quad (6d)$$

$$\text{and } \bar{v}_x = x_b/P \quad (6e)$$

which may be also written in terms of the Equations 6a to c. (We designate here as Scatchard hydration all protein-water interactions characterized by multiple equilibria. Another type of water binding, preferential hydration, will be encountered further on. For a particularly clear exposition of the relationships between these concepts, see Reference 29.)

The concentrations are commonly expressed in moles per liter but may, when more convenient, equally well be expressed in moles per 1000 g water, as will be the case in the following. While this will change the numerical values and dimensions of association constants, \bar{v}_w and \bar{v}_x will remain unaffected. Strictly speaking, all terms should be expressed as the corresponding activities rather than as molar or molal concentrations. (However, in view of the generally large molecular weights of proteins, even fairly concentrated solutions are usually no more than $10^{-13} M$ and, under the conditions of many experiments, virial coefficients are negligible, i.e., the protein has a very small net charge. Deviations from this assumptions will be discussed specifically later.)

The experimentally derived quantity to be considered is the slope of the plot of either the spin-lattice (R_1) or the spin-spin (R_2) relaxation rate of the water vs. the concentration of protein present. In analogy to other quantities encountered in solution theory, the slope $(dR/dP)_\mu$ may be termed the relaxation increment; the subscript μ indicates that solutions are at constant chemical potential and, in terms of experimental procedure, that exhaustive dialysis against buffer was performed prior to the proton NMR relaxation measurements.

Considering now the relaxation increment of an aqueous solution of protein in the presence of salt as a concentration-dependent function, and expressing the total relaxation rate of the water in the three-component system in terms of the solution components, one may write, on the basis of fast exchange of water between two fractions of rates R_b (for bound water) and R_f (for free water), and in view of Equation 6b,

$$R = \frac{w_b}{W} R_b + \frac{w}{W} R_f = \frac{(p \sum \sum_i K_{ij} w^i x^j) R_b + w R_f}{p \sum \sum_i K_{ij} w^i x^j + w} \quad (7)$$

From R as a function of P , W , and X , one has the total derivative

$$\left(\frac{dR}{dP} \right)_\mu = \left(\frac{\partial R}{\partial P} \right)_{w,x} + \left(\frac{\partial R}{\partial W} \right)_{p,x} \left(\frac{dW}{dP} \right)_\mu + \left(\frac{\partial R}{\partial X} \right)_{p,w} \left(\frac{dX}{dP} \right)_\mu \quad (8)$$

The coefficients of the three terms can be evaluated by partial differentiation of Equation 7 with the use of Equations 6a to c. More directly, from Equations 7 and 5b (where w , because of the exhaustive dialysis, is a constant),

$$R = \frac{(W - w)R_b + wR_f}{W} = R_b - (R_b - R_f) \frac{w}{W} \quad (9)$$

and from this,

$$\left(\frac{\partial R}{\partial P}\right)_{w,x} = 0, \quad \left(\frac{\partial R}{\partial W}\right)_{p,x} = \frac{(R_b - R_r)w}{W^2}, \quad \left(\frac{\partial R}{\partial X}\right)_{p,w} = 0 \quad (9a)$$

and, therefore,

$$\left(\frac{dR}{dP}\right)_{\mu} = \left(\frac{\partial R}{\partial W}\right)_{p,x} \left(\frac{dW}{dP}\right)_{\mu} = \frac{(R_b - R_r)w}{W^2} \left(\frac{dW}{dP}\right)_{\mu} \quad (10)$$

From Equations 5b and 6d, $W = w + w_b = w + \bar{v}_w P$ and, with $dw/dP = 0$,

$$\left(\frac{dW}{dP}\right)_{\mu} = \bar{v}_w \quad (11)$$

Since $w_b \ll W$ implies $w \cong W$ ($\cong 55.6$), Equation 10 becomes

$$\left(\frac{dR}{dP}\right)_{\mu} = \frac{R_b - R_r}{W} \bar{v}_w \quad (12)$$

Because protein molecular weights are not always precisely known, it is convenient to replace the molality P by the concentration c (in grams of protein per grams of water) and the hydration \bar{v}_w (in moles per mole) by \bar{v}'_w (in the conventional units of grams bound water per gram protein). Then $c = PM_p/1000$ and $\bar{v}'_w = \bar{v}_w M_w/M_p$, where M_p and M_w are the molecular weights of protein and water, respectively. Also, $dP/dc = 1000/M_p$ and, $1000/WM_w$ being unity,

$$\left(\frac{dR}{dc}\right)_{\mu} = \left(\frac{dR}{dP}\right)_{\mu} \left(\frac{dP}{dc}\right) = (R_b - R_r) \bar{v}'_w \quad (13)$$

In the cited work,²⁴ the relationship of R to c (as shown in Figure 1 for both R_1 and R_2 results) was linear. One may write Equation 9 alternatively as

$$R = R_r + (R_b - R_r) \frac{w_b}{W} = R_r + (R_b - R_r) \frac{P \bar{v}_w}{W} = R_r + (R_b - R_r) c \bar{v}'_w \quad (13a)$$

and from Equations 13 or 13a, with a constant relaxation increment,

$$(dR/dc)_{\mu} = (R_b - R_r) \bar{v}'_w = k \quad (13b)$$

or

$$R = R_r + (R_b - R_r) c \bar{v}'_w = R_r + kc \quad (13c)$$

Absence of such linearity might be due to polydispersity and consequent changes in the $(R_b - R_r)$ factor, which would have to be allowed for. The other factor in the relaxation increment, \bar{v}'_w , is generally taken to be independent of protein concentration (see Reference 30). If it is not actually constant, an additional term accounting for its concentration dependence would have to be included in Equations 13b and c, unless a change from concentration units to activities will remove the nonlinearity, as discussed in Section III.A.2.

If it is desired to express protein concentrations as c_2 in grams protein per milliliter solution, the solution density ρ and the concentration of the third component, c_3 , need to be known, whereupon

$$c = \frac{c_2}{\rho - c_2 - c_3} \quad (14)$$

$$\text{and} \quad \left(\frac{dR}{dc_2}\right)_\mu = k \frac{\rho - c_3}{(\rho - c_2 - c_3)^2} \quad (14a)$$

The need to know solution densities may be eliminated for all except very high protein concentrations with a knowledge of the partial specific volume \bar{v} and the solvent density ρ_0 . From the definition of \bar{v} , it can then be shown that

$$c = \frac{c_2}{\rho_0(1 - \bar{v}c_2) - c_3} \quad (14')$$

$$\text{and} \quad \frac{dR}{dc_2} = k \frac{\rho_0 - c_3}{[\rho_0(1 - \bar{v}c_2) - c_3]^2} \quad (14'a)$$

In cases of high protein concentration, the more general Equations 14 and 14a may have to be used. At low protein concentration, where $\rho_0 > 1.0$ while $c_2, c_3 \ll \rho$, Equations 14a and 14'a reduce to expressions formally identical to Equation 13b with c_2 in place of c ; a corresponding remark is true for Equations 14 and 14' with respect to Equation 13c. From Equation 13b, $R_b = k/\bar{v}'_w + R_i$ for either R_i or R_{2f} , and, therefore,

$$R_{2b}/R_{1b} = (k_2 + R_{2f} \bar{v}'_w)/(k_1 + R_{1f} \bar{v}'_w) \quad (15)$$

However, generally $R_i \bar{v}'_w \ll R_b$; hence, from the definition of k , one obtains the useful approximation

$$R_{2b}/R_{1b} \approx k_2/k_1 \quad (15a)$$

The parameters k_1 , R_{1f} , k_2 , and R_{2f} are experimentally accessible as the slope k and intercept R_i from R_i or R_{2f} vs. c_2 plots, respectively, such as those of Figure 1.

C. Evaluation of Data

Use of these relationships in conjunction with the Kubo-Tomita-Solomon equations,^{31,32} which relate R_{1b} and R_{2b} to the correlation time of the bound water, will give the requisite number of equations to permit simultaneous solution for \bar{v}'_w and τ_c . These equations may be written as

$$R_{1b} = 2K\tau_c[(1 + \omega_0^2\tau_c^2)^{-1} + 4(1 + 4\omega_0^2\tau_c^2)^{-1}] \quad (16a)$$

and

$$R_{2b} = K\tau_c[3 + 5(1 + \omega_0^2\tau_c^2)^{-1} + 2(1 + 4\omega_0^2\tau_c^2)^{-1}] \quad (16b)$$

where $\omega_0 = 2\pi\nu_0$ is the nuclear angular precessional frequency for the nuclide observed, in radians per second, and K is a measure of the strength of the nuclear interaction, i.e.,

$$K_{\text{deuterons}} = (3/80)(e^2qQ/\hbar)^2(\eta^2/3 + 1)^{-1}S_{\text{deut}}^2 \quad (16c)$$

and

$$K_{\text{protons}} = (3/20)\hbar^2\gamma^4\tau^{-6}S_{\text{prot}}^2 \quad (16d)$$

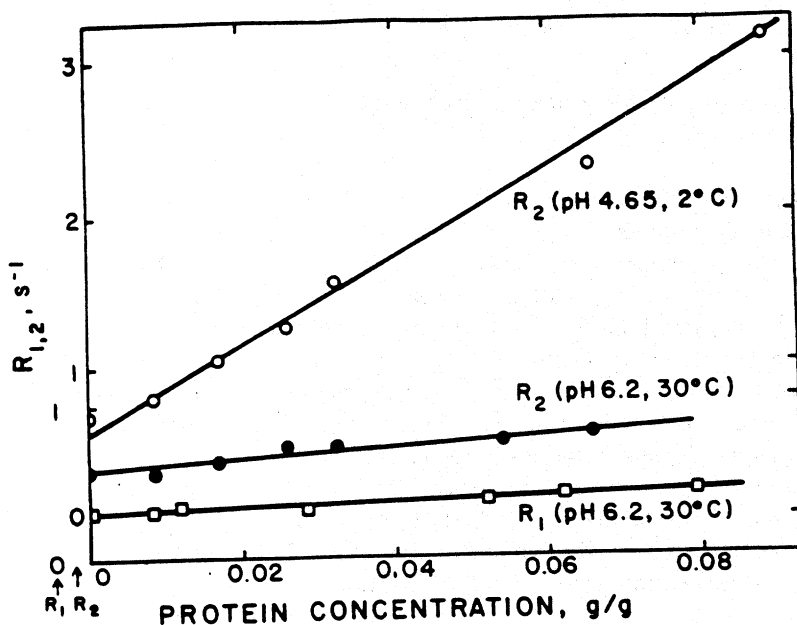


FIGURE 1. Dependence of proton relaxation rates on β -Lg A concentrations (g protein per gram water) in H₂O. Transverse relaxation rates R_2 at pH 4.65 and 2°C (○-○-) and at pH 6.2 and 30°C (●-●-). Longitudinal relaxation rates R_1 (□-□-) at pH 6.2 and 30°C (shown for comparison only; not used in calculations). Points represent experimental values; lines represent least-squares fits. All points show linear relationship of relaxation rates to concentration at pH 4.65 and 6.2. (From Kumosinski, T. F. and Pessen, H., *Arch. Biochem. Biophys.*, 218, 286, 1982.)

Here e is the electronic charge, 1.6022×10^{-19} C, q is the electric field gradient, Q is the nuclear electric quadrupole moment, \hbar is Planck's constant divided by 2π , 1.0546×10^{-27} erg·s; η is a dimensionless parameter measuring the deviation from axial symmetry;³³ γ is the gyromagnetic ratio for the proton, 2.6752×10^4 rad-Gauss⁻¹s⁻¹; r is the internuclear proton distance for water, 0.1526 nm; and S_{deut} and S_{prot} are respective order parameters.⁷ It may be noted that these expressions assume no particular model for the relaxation mechanism accompanying NMR hydration. The thermodynamic theory can be used whether isotropic relaxation ($S = 1$) or anisotropy of the bound water ($S < 1$) is hypothesized, where in the latter case the "bound" should be understood in the sense of "hydrodynamically influenced layers" or "surface-induced probability distribution of water molecules".^{7,34,35} The above treatment can easily be extended to a model postulating three or more states.

III. RELAXATION: ²H NMR

The nuclide chosen for these particular studies²⁴ was deuterium. Its use eliminates the effect of cross relaxation of water protons with protein protons, which had been shown by Edzes and Samulski³⁶ to have a significant effect on spin-lattice relaxation rates of water protons with varying protein concentrations.

A. Influence of Protein Hydrophilic Self-Association: β -Lactoglobulin A

The previously derived relationships were tested on bovine β -lactoglobulin A (β -Lg A), the major whey protein in milk, under various environmental conditions. At pH 5, β -Lg A exists as a dimer of molecular weight 36,200. At pH 4.65, β -Lg A undergoes a dimer-to-octomer self-association involving hydrophilic groups. ²H NMR relaxation measurements made at the above

conditions served to test whether the notion of increased hydration with increasing hydrophilic self-association is valid.

1. Experimental Procedures

a. Preparation of Solutions

The following procedures are described to illustrate methods that have led to satisfactory results in studies of β -Lg in solution.²⁷ Protein solutions to be used for proton resonance measurements, prepared 1 d before use, were exhaustively dialyzed overnight against buffer at 0 to 5°C: dilutions for the concentration series to be studied were made with the appropriate dialyate. Solutions to be used for deuterium resonance measurements were made up from a stock solution prepared by partial deuterium exchange. A suitable amount of crystalline protein in a stoppered vial was allowed to equilibrate repeatedly for 24-h periods at 4°C as a slurry with a small quantity of D₂O, followed by high-speed centrifugation and addition of fresh D₂O, for a total of five times. The solutions were buffered by direct addition of solid potassium phosphate, and the pH was adjusted by addition of 0.1 *N* NaOD in D₂O. Concentrations of β -Lg were determined spectrophotometrically from an absorption coefficient of 0.96 ml·mg⁻¹·cm⁻¹ at 278 nm.³⁷

b. Relaxation Measurements

Resonance relaxation spectra were obtained by pulse Fourier transform spectroscopy with a JEOL FX60Q spectrometer operating at a nominal frequency of 60 MHz. The frequency of observation for protons was 59.79 MHz; for deuterons, 9.17 MHz. Raw data were in the form of relative intensities as calculated by the JEOL 980B computer.

Since the high concentration of water in a dilute solution produces an intense signal, a single accumulation at the particular sample temperature (2, 10, or 30 ± 1°C) was sufficient for each spectrum. Even then, care was necessary to avoid exceeding the dynamic range of the computer with consequent truncation. To this end, as well as to economize on the limited amount of the A variant of the protein available, small sample volumes were employed by use of a microcell assembly with an expendable 35- μ l sample bulb, available from Wilmad Glass Company, Inc. The protein solution was introduced very slowly into the spherical bulb by means of a fine-gauge syringe needle inserted through its capillary neck, to avoid the inclusion of any air bubbles. Bubbles trapped below the neck could lead to vortex formation in the spinning sample bulb and vitiate the necessary assumption of spherical sample geometry.

The bulb, suspended by its neck from a chuck attached to a plastic cap, was positioned snugly inside a precision 5-mm OD sample tube which, initially, contained also the lock-signal solvent. The small amount of this solvent in the residual annular space outside the bulb was not always sufficient to assure maintenance of the lock; occasional failure of the lock during a lengthy series of automatic measurements resulted in loss of usable data. A second arrangement was then used in which the 5-mm tube, containing the sample bulb but no solvent, was positioned by means of fluorocarbon plastic spacers concentrically within a precision 10-mm OD sample tube accommodating a much larger quantity of lock-signal solvent. Incidental advantages of this arrangement were that the outside of the sample bulb was thus kept dry, and that the solvent could be sealed within the annular space between the two tubes and so kept from contamination for a greatly extended time. Except for these advantages, either arrangement resulted in the same measurements. The cell assembly, in either case, was positioned in the JEOL FX60Q 10-mm ¹H/¹³C dual probe insert.

Longitudinal (spin-lattice) relaxation rates R_1 were measured by the inversion-recovery method,³⁸ where the repetition time T in the pulse sequence [... T ... π ... τ ... $\pi/2$...] was chosen to be at least five times T_1 ($\cong R_1^{-1}$) and the values of the variable delay time τ ranged from 10 ms to 3 s, for a total of between 5 and 20 τ -values, depending on the detail desired. From the Bloch equations³⁹ under the conditions of this method, the relation of the peak intensity A_i to the pulse delay time τ becomes

$$A_\tau = A_\infty [1 - 2 \exp(-R_1 \tau)] \quad (17)$$

where A_∞ is the limiting peak intensity for $\tau \rightarrow \infty$. Independent measurement of A_∞ , a source of irreducible error, can be dispensed with, and the problem of weighting the data points in the conventional linear plot (logarithm of a function of relative peak heights vs. τ) can be eliminated, by fitting directly to the data points (τ, A_τ) by least-squares an exponential of the form of Equation 17, from which the two parameters A_∞ and R_1 can be obtained.

The factor 2 preceding the exponential in Equation 17 is based on theory which predicts $A_\infty = -A_0$, where A_0 is the peak intensity for $\tau = 0$. It is recognized that in point of fact this equality rarely holds exactly because of slightly imperfect adjustment of the flip angle π . When Equation 17 is used in its logarithmic form, A_∞ must be determined by explicit measurement, and A_0 then is usually seen, from the ordinate intercept of the straight-line plot of $\ln(A_\infty - A_\tau)$ vs. τ , to differ somewhat from its theoretical value. This, however, is essentially without relevance with respect to the only parameter of intrinsic interest, namely the R_1 obtained from the slope, except possibly insofar as agreement of the intercept with $\ln 2A_\infty$ would be some measure of the quality of the data as a whole.

When the equation is used, as it was here, in the exponential form with A_∞ not explicitly determined, the assumption $A_\infty = -A_0$ implies a two-parameter exponential fit, whereas $A_\infty \neq -A_0$ would imply a three-parameter exponential fit. The latter has been advocated or practiced in the past by various authors.⁴⁰⁻⁴³ Such a practice, however, has ignored the definitive treatment of this matter by Leipert and Marquardt,⁴⁴ concurred in by Becker et al.,⁴⁵ which has shown conclusively that introduction of a third adjustable parameter, so far from improving the statistics, leads to a significant loss of precision in the estimate of R_1 because of an undesirable correlation between what should be statistically independent parameters, R_1 and A_∞ . The effect, on the other hand, of even a considerably misadjusted flip angle on the value of R_1 obtained was shown to be insignificant for values of $R_1 > 0.1$ s, a condition generally satisfied.

The fitting of the two-parameter exponential was carried out by computer by means of an iterative program. For each sample, R_1 was determined at least four times and the results were averaged. This procedure was repeated at each concentration; a minimum of six concentrations were used under each set of conditions of temperature and pH at which the resonance relaxation of each nuclide was examined.

Transverse (spin-spin) relaxation rates R_2 were determined by spin-locking measurement⁴⁶ of $R_{1\rho}$, the longitudinal relaxation rate in the rotating frame. R_1 equals R_2 in dilute solutions of low viscosity whenever the magnitude of $R_{1\rho}$ is independent of $H_{1\rho}$, the spin-locking radio-frequency field in the rotating frame; this was the case, within the limits of experimental error, in this work. R_2 was evaluated as described above for R_1 , except that the relation between peak intensity A_τ and decay time τ derived from the Bloch equations in this case³⁹ becomes

$$A_\tau = A_0 \exp(-R_2 \tau) \quad (18)$$

where the initial intensity A_0 replaces A_∞ as the maximum peak intensity. Again, a least-squares two-parameter exponential fit to the data points was performed by an iterative computer program, from which A_0 and R_2 were obtained.

For each sample, R_2 was determined with the same number of replications as R_1 . Measurements of one mode of relaxation were made on the identical samples and immediately following the completion of measurements of the other mode, or at latest the next day. In this manner, measurements for proton relaxation at 59.75 MHz were made at pH 6.2 at 2 and 30°C, at pH 4.65 at 2 and 30°C, and at pH 2.7 at 10°C. Measurements for deuteron relaxation at 9.17 MHz were made at pH 6.2 and 4.65, both at 2 and 30°C.

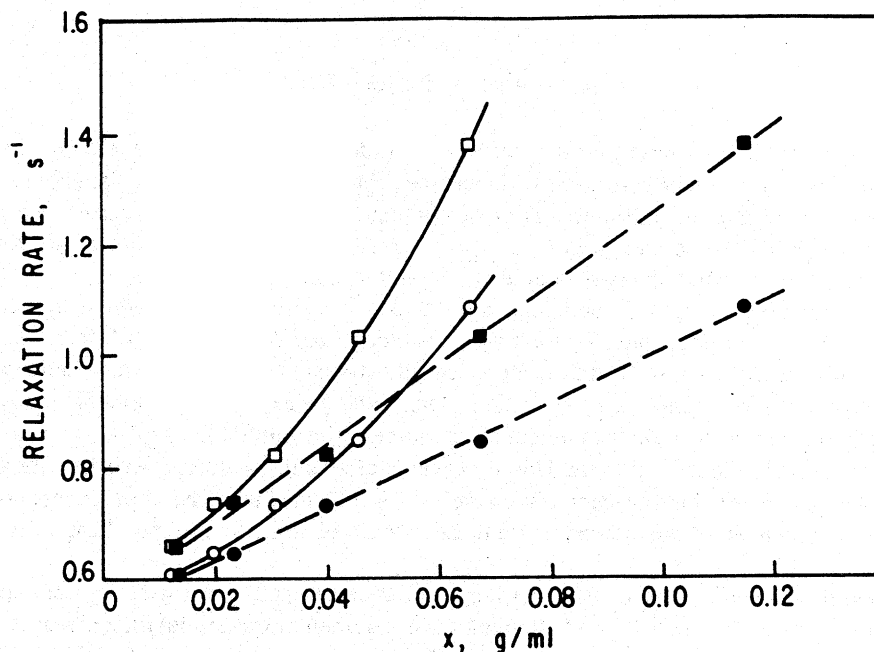


FIGURE 2. Dependence of water proton relaxation rates of b-Lg A on both concentration and activity, at pH 2.7 and 10°C. Transverse relaxation rates (squares) as function of X (-□-□-), concentration and (-■-■-), activity. Longitudinal relaxation rates (circles) as function of X (-○-○-), concentration and (-●-●-), activity. All points represent experimental values; lines represent least-squares polynomial fits of highest degree to make a statistically significant contribution to goodness of fit (F-test). Dependence on concentration is found to be of second degree as consequence of charge effects at pH 2.7. (Polynomial coefficients for R_1 , $a_0 = 0.562$, $a_1 = 2.926$, and $a_2 = 75.86$; for R_2 , $a_0 = 0.606$, $a_1 = 3.468$, and $a_2 = 125.9$.) Activities take these effects into account, and dependence on activities is linear. (Coefficients of straight line: for R_1 , $a_0 = 0.541$, $a_1 = 4.691$; for R_2 , $a_0 = 0.560$, $a_1 = 7.061$). (From Kumosinski, T. F. and Pessen, H., *Arch. Biochem. Biophys.*, 218, 286, 1982.)

2. Analysis of Data

a. Activities and the Multicomponent Expression

At this point, an observation regarding predictions resulting from the derived multicomponent expressions above may be in order. Since these are based ultimately on equilibrium constants, the mass terms should be properly expressed as activities instead of concentrations. Consequently, relaxation rate vs. concentration curves should be expected to be nonlinear whenever there are appreciable protein activity coefficients. Figure 1 shows concentration dependences of R_1 and R_2 for β -Lg A at pH 6.2 and 30°C, and of R_2 at pH 4.65 and 2°C. Under these conditions, the charge-to-mass ratio and the second virial coefficient are relatively small ($B_0 = 0.9$ ml/g).³⁷ In fact, all these data exhibit linear relationships over a concentration range from 0 to 0.08 g protein per gram water, where γ does not differ greatly from unity. Figure 2, on the other hand, shows corresponding plots for pH 2.7 and 10°C, where the net charge is approximately 40 and the second virial coefficient is 8.5 ml/g.⁴⁷ The plots in terms of concentration here are clearly nonlinear. A change in the concentration scale to grams protein per gram water had no significant effect on the nonlinearity of the plots. (Low-temperature data were used at this pH for experimental reasons: the protein under these conditions undergoes a dissociation from dimer to monomer, but at low temperature, the amount of monomer at concentrations in excess of 0.01 g/ml is negligible.⁴⁷)

A polynomial curve-fitting program was used with all data on Figures 1 and 2, as well as all other concentration-dependent data, in order to determine linearity or nonlinearity, the degree of the polynomial being determined by goodness of fit as judged by the standard F-test. (The

regression program used selects the lowest-degree expression for which the sum of squares due to the addition of one higher degree is statistically insignificant.) The two concentration plots of Figure 2 give polynomials of degree two. Protein concentrations, c , were then transformed into activities, a , by means of the relationship $a = \gamma c$, where the activity coefficient $\gamma = \exp(2B_0 c)$ was obtained (see Equation 2) from the second virial coefficient $B_0 = 8.5$ ml/g. as cited above. Activity plots corresponding to the concentration plots are also shown in Figure 2; it is evident that these are linear by the same criteria.

Under the conditions of Figure 2, γ is sensibly larger than unity and, even in the presence of salt, failure to treat R as a function of activity rather than concentration will evidently lead to excessively high values of hydration (see Equation 13c). The opposite would be true under conditions when, in the absence of salt, charge fluctuations and consequent intermolecular attraction exist. With γ less than unity, a concentration plot in place of the correct activity plot for R must lead to inordinately low values of hydration. Alternatively, protein concentrations could continue to be used, provided the right-hand side of Equation 13 is multiplied by $(da/dc)_\mu$.

These results may be taken to demonstrate the validity of the multicomponent expression. This expression is used in the following in analyzing the data to describe the hydration of the genetic A variant of β -Lg, under nonaggregation conditions, as well as under the well-characterized dimer-to-octamer association.⁴⁸⁻⁵² (This phenomenon, because it involves a four-fold association of dimer under conditions where dissociation to monomer is negligible, is referred to in the following as "tetramerization".) It has been demonstrated that here the virial coefficients are small,^{37,47} so that it is permissible to simplify the treatment by using protein concentrations.

b. Isotropic Binding, Two-State Model

i. Determination of Correlation Times

Proton spin-spin relaxation measurements of water in solutions of β -Lg A gave results indicating a single relaxation rate, whereas spin-lattice results could be fitted only by the sum of two exponential functions (Figure 3A). This behavior is consistent with the work of Edzes and Samulski³⁶ and others,^{26,53} who found a cross relaxation mechanism between water protons and protein protons to make a significant contribution to the spin-lattice relaxation rate in water-collagen systems. Subsequently, Koenig et al.⁵⁴ showed that cross relaxation also exists in spin-lattice relaxation (T_1 processes) in globular protein solutions, i.e., the cross-relaxation rate disperses as a T_1 process and not as a T_2 process. For the solution illustrated in Figure 3A, with the notation of Edzes and Samulski, the parameters in the equation $m(t) = c^+ \exp(-R^+ t) + c^- \exp(-R^- t)$ are $R^+ = 15.0$, $R^- = 0.45$, $c^+ = 0.01$, and $c^- = 1.01$, where the reduced magnetization $m(t) \equiv (A_{\infty} - A_t)/2A_{\infty}$. The statistics here were poor because of instrumental limitations.⁵⁵ (Cross relaxation, calculated for β -Lg in a novel way,⁸ was found to contribute to the observed apparent spin-lattice relaxation to the extent of about 90%.) As an alternative approach, protein solutions were made up in D_2O , and the dependence of both R_1 and R_2 on protein concentration was measured by deuterium NMR at 9.17 MHz which, in effect, eliminated cross relaxation from the T_1 measurements (Figure 3B). The concentration dependence of R_2 of protons in solutions of β -Lg A in H_2O under the same environmental conditions was also measured (see Figure 1).

Concentration plots of R_1 and R_2 for D_2O (Figure 4) showed no evidence of nonlinearity, at either pH and either temperature, over the concentration range studied. This agrees with the low virial coefficient of β -Lg A under these conditions.³⁷ The relaxation increments k_1 and k_2 , together with the corresponding intercepts R_{1f} and R_{2f} (Figure 4), were used in Equations 13 and 16 to determine the bound-water correlation times τ_c shown in Table 1. As can be seen, τ_c increased as the temperature decreased; this is in quantitative agreement with the requirement of Stokes' equation that τ_c increase with both increasing viscosity and decreasing temperature. Furthermore, τ_c also increased when the pH was lowered from 6.2 to 4.65, as would be predicted from the work of Timasheff and Townend,⁵⁶ which showed that β -Lg A associates at the lower, but not at the higher pH, and that the association increases with decreasing temperature.

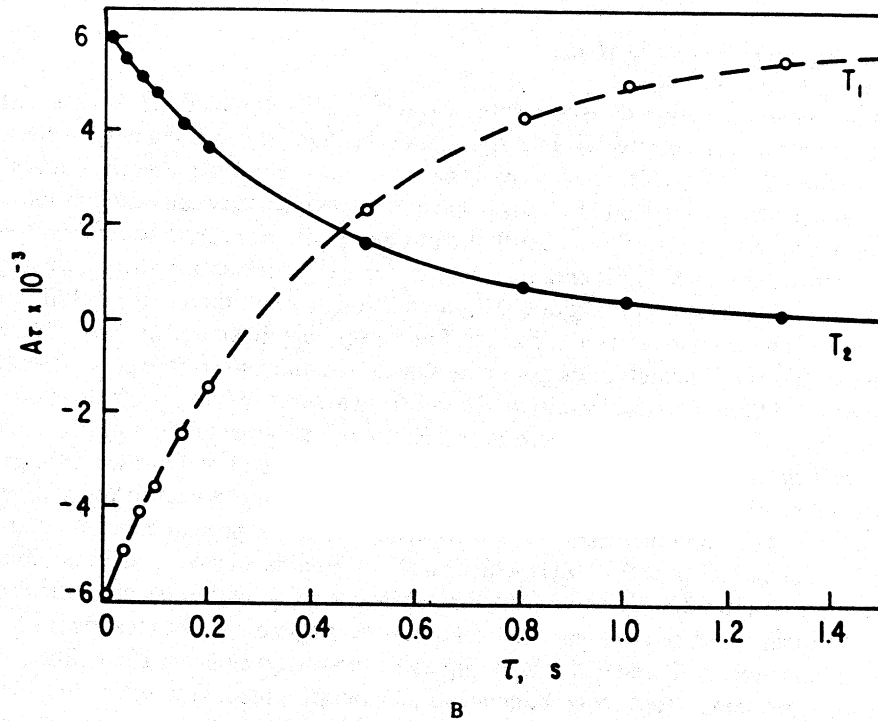
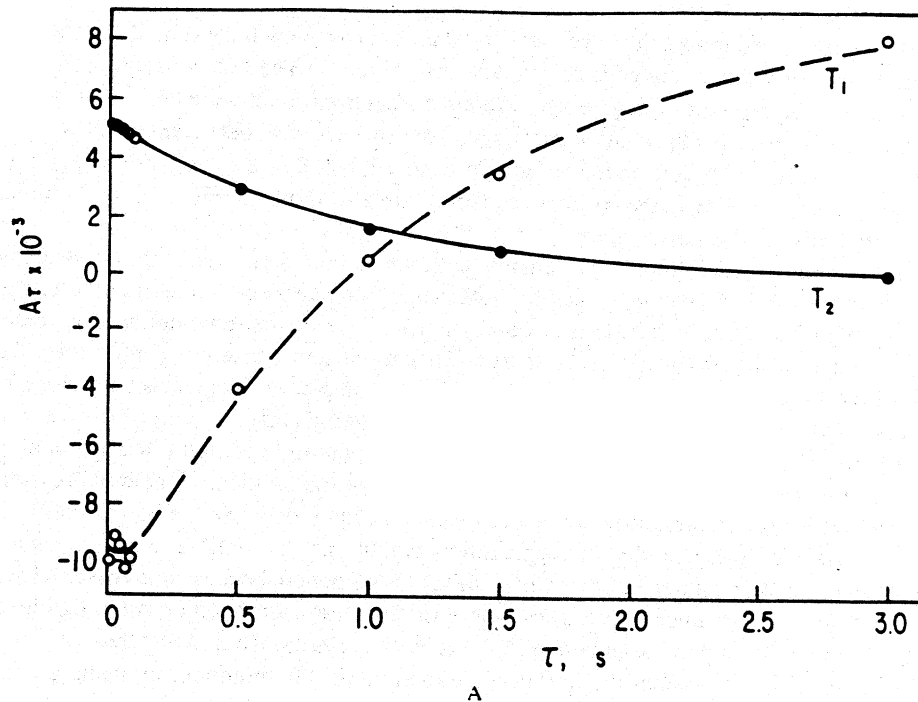


FIGURE 3. (A) Proton resonance peak intensities A as functions of time t , for solutions of β -Lg A in H_2O (6.09×10^{-2} g protein per gram H_2O) at pH 6.2, 30°C . Intensities for transverse relaxation (T_2 , $\bullet\text{---}\bullet$) as function of decay time, from spin-locking measurements of $T_{1\rho}$; intensities for longitudinal relaxation (T_1 , $\text{---}\circ\text{---}$) as function of delay time, from inversion-recovery measurements. Points represent experimental values. Line for T_2 represents two-parameter exponential fit. Line for T_1 represents four-parameter double-exponential fit; need for this fit shown by initial course of this line, indicative of cross relaxation. (B) Deuteron resonance peak intensities A as function of time t , for solutions of β -Lg A in D_2O (2.86×10^{-2} g protein per gram D_2O) at pH 6.2, 30°C . In this case, the indication of cross relaxation in T_1 is absent and a two-parameter exponential shows excellent fit to the experimental points even at shortest times. (From Kumosinski, T. F. and Pessen, H., *Arch. Biochem. Biophys.*, 218, 286, 1982.)

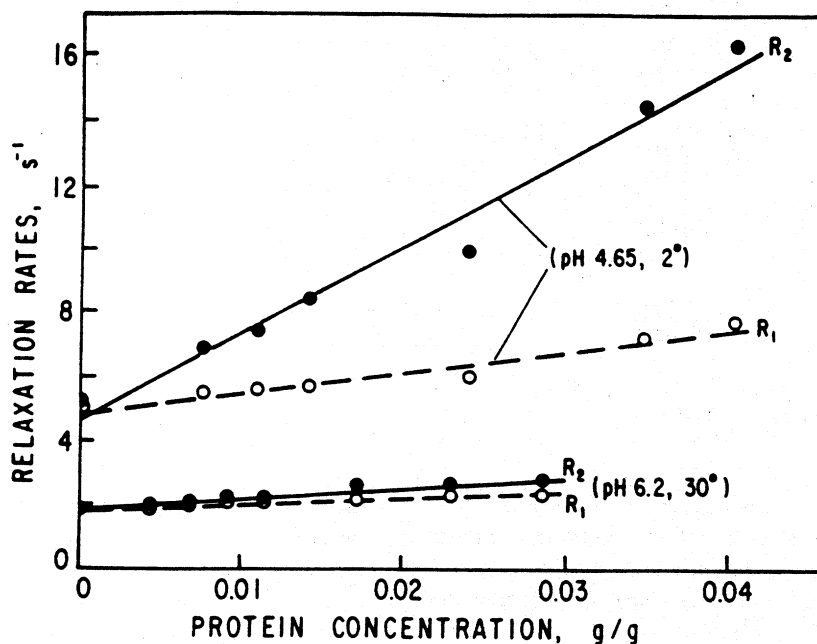


FIGURE 4. Dependence of deuteron relaxation rates on β -Lg A concentrations (g protein per gram water) in D₂O. Transverse relaxation rates R_2 (-●-●-) at pH 4.65, 2°C and at pH 6.2, 30°C. Longitudinal relaxation rates R_1 (-○-○-) under the same two sets of conditions. Points represent experimental values; lines represent least-square fits. Points at all concentrations show linear relationship of relaxation rates to concentration, at both sets of pH and temperature conditions, and for both modes of relaxation. (From Kumosinski, T. F. and Pessen, H., *Arch. Biochem. Biophys.*, 218, 286, 1982.)

Table 1
DEUTERON NMR RELAXATION AND HYDRODYNAMIC RESULTS
FOR β -LACTOGLOBULIN IN SOLUTION^a

pH	T (°C)	k_1^a	k_2	R_{1f} (s ⁻¹)	R_{2f} (s ⁻¹)	τ_c (ns)	r_{NMR}^b (nm)	r_{sed} (nm)	$(\tau_c)_{calc}$ (ns)
6.2	30	20.7 ±0.9	31.9 ±1.9	1.93 ±0.01	1.93 ±0.04	10.0 ±2.7	2.32 0.19	2.70	10.2
	2	17.9 ±2.1	58.9 ±5.2	5.46 ±0.24	5.25 ±0.28	25.6 ±4.1			22.5
4.65	30	25.4 ±1.9	73.2 ±5.0	2.01 ±0.04	1.79 ±0.12	22.5 ±3.3	3.04 ±0.15	4.35	65.9
	2	63.9 ±7.1	274.2 ±19.0	4.90 ±0.16	4.67 ±0.44	32.2 ±4.6			145.0

Adapted from Reference 27.

Error terms in this and subsequent tables represent the standard error of the parameter.

Spherical model assumption.

ii. Determination of Hydration Parameters

Since the extent of a possible intermolecular contribution, R'_{2b} , to the spin-spin relaxation of bound-water protons and the number of protein protons so contributing are unknown, determination of Scatchard hydrations was attempted by three different methods and the results were compared.

$$(e^2qQ/h) = 215.6 \text{ kHz}^{a,b}$$

pH	T (°C)	\bar{v}'_w (g H ₂ O per g protein)	ΔG (kcal)	$-\Delta H$ (kcal)	$-\Delta S$ (e.u.)
6.2	30	0.0063 ±0.0008	0.90 ±0.08		
	2	0.0072 ±0.0020	0.74 ±0.15	0.8 ±3.0	6 ±10
4.65	30	0.0095 ±0.0002	0.65 ±0.01		
	2	0.0301 ±0.0003	-0.044 ±0.006	6.9 ±1.6	24.8 ±5.8

^a Adapted from Reference 27.

^b Method I, as described in Section III.A.2.b.

Method I — Only the deuterium NMR relaxation increments were used, with a value of $e^2qQ/h = 215.6 \text{ kHz}^{57}$ and with the asymmetry parameter η assumed to be zero. This type of calculation gives low values of \bar{v}'_w , as shown in Table 2; however, low values could be expected because the relaxation increment probably samples only a percentage of the total hydration of a protein, since at 9.17 MHz any bound water with τ_c values less than 6 ns would have a T_1/T_2 ratio of unity. At pH 4.65, where tetramerization occurs, the hydration markedly increases with decreasing temperature, whereas at pH 6.2, where none occurs, the hydration is lower and independent of temperature. This is consistent with the findings of Timasheff and co-workers^{48,58} from small-angle X-ray scattering that the geometry of the octamer must include a large central cavity in which trapped water could reside.

Method II — A combination of the τ_c values found by deuterium NMR at 9.17 MHz (Table 1) and the k_2 values found from proton NMR at 59.75 MHz was used (see Figure 1). The reason for this procedure is that the quadrupole coupling constant for the bound water should actually decrease as hydrogen bonding increases.⁵⁹ Here R_{2b} can be calculated from Equation 16b at 59.75 MHz, and the \bar{v}'_w values can be easily obtained from the simple relationship $\bar{v}'_w = k_2/(R_{2b} - R_{2f})$, derived from Equation 13b. Such hydration values (Table 3) are slightly higher than those from deuterium relaxation measurements only (Table 2), but show the same temperature and pH dependence. (Combination experiments of this kind would be best performed at the same Larmor frequency; however, the availability of only a single spectrometer with no variable frequency capability would preclude this possibility. These experiments could shed light on such problems as the constancy of the hydrogen-bond distance under various conditions and the existence of a distribution of correlation times in the total hydration shell.)

Method III — This is a combination procedure also, with an extra intermolecular interaction term R'_{2b} added to the proton spin-spin relaxation rate R_{2b} . Based on the small-angle X-ray scattering results for β -Lg A of Witz et al.,⁴⁸ in conjunction with the known molecular weight and amino acid composition, a simple consideration of the molecular geometry shows that, on the average, each proton in the protein will have six neighboring protons at a distance of 0.261 nm. From this average intermolecular distance, together with the τ_c values of Table 1 and the relationship $\bar{R}_{2b} = R_{2b} + 12 R'_{2b}$ (where \bar{R}_{2b} is the total spin-spin relaxation rate), the hydration can be calculated as $\bar{v}'_w = k_2/(\bar{R}_{2b} - R_{2b})$. These values (Table 3) are in close agreement with those in Table 1. Altogether, no great difference exists in the \bar{v}'_w values from all three methods.

Table 3
HYDRATION AND THERMODYNAMICS FOR β -LACTOGLOBULIN DERIVED FROM τ_c VALUES OF TABLE 1 BY METHODS II AND III^a

pH	T (°C)	k_2	R_{2r} (s ⁻¹)	R_{2b} (s ⁻¹)		v'_w (g H ₂ O per gram protein)		ΔG (kcal)		$-\Delta H$ (kcal)		$-\Delta S$ (e.u.)	
				II ^b	III ^c	II ^b	III ^c	II ^b	III ^c	II ^b	III ^c	II ^b	III ^c
6.2	30	3.5	0.34	228	337	0.0152	0.0103	0.35	0.59				
		± 0.5	± 0.02			± 0.0021	± 0.0007	± 0.07	± 0.04	0	0	1.2	1.9
	2	8.1	0.70	530	784	0.0152	0.0103	0.32	0.54				
		0.4	± 0.02			± 0.0008	± 0.0014	± 0.03	± 0.07			± 0.2	± 0.1
4.65	30	9.2	0.27	468	694	0.0197	0.0133	0.20	0.43				
		± 0.8	± 0.04			± 0.0016	± 0.0011	± 0.05	± 0.04				
	2	28.2	0.56	660	978	0.0428	0.0289	-0.25	-0.032	4.62	4.62	15.9	16.7
		± 1.1	± 0.05			± 0.0017	± 0.0011	± 0.02	± 0.021	± 0.73	0.70	± 2.6	± 2.4

^a Adapted from Reference 27.

^b Method II uses τ_c from Table 1 and proton k_2 .

^c Method III uses, in addition to the procedure of Method II, the assumption $\bar{R}_{2b} = R_{2b} + 12 R'_{2b}$, with the intermolecular proton distance for β -Lg A calculated from the partial specific volume as 0.261 nm, as described in Section III.A.2.

iii. Comparison of Results with Other Structural Information

Dynamics of β -Lg dimer — With the τ_c values calculated from k_2/k_1 from deuterium NMR spin-spin and spin-lattice relaxation increments, dR_2/dc and dR_1/dc , a Stokes radius r_{NMR} for the bound water can be calculated from the Stokes-Einstein relation⁶⁰ on the basis of a spherical model (Table 1). At pH 6.2, where β -Lg A exists as the unassociated dimer, the value of r_{NMR} is slightly lower than the one for the protein itself derived from hydrodynamic data, r_{sed} .⁶¹ This discrepancy could be due to the spherical approximation inherent in the use of the Stokes-Einstein equation, inasmuch as the β -Lg dimer actually has an axial ratio of approximately 2:1.³⁷ Moreover, the Stokes radius of the protein obtained from sedimentation includes the water of hydration and should, therefore, be larger than the Stokes radius of the bound water calculated from the ^2H NMR relaxation data. What should be compared with the τ_c of the bound water is the τ_c of the protein without any contribution from hydration. For the latter, values of 10.2 ns at 30°C and 22.5 ns at 2°C (Table 1) can be calculated for the protein with the use of its partial specific volume, 0.751 ml/g, and an asymmetry factor of 1.168⁶² to account for the dimer axial ratio of 2:1. These values are in excellent agreement with the experimental τ_c of the bound water at pH 6.2 at 30°C and 2°C (see Table 1).

Hydration and dynamics of β -Lg octamer — At pH 4.65, where the protein exists to a large extent as the octamer even at 30°C at concentrations above 0.01 g/ml,⁴⁹ the Stokes radius of the bound water is about 30% less than the Stokes radius of the octamer itself. However, this value is still much closer to the theoretical value than those obtained by other investigators for other proteins.^{5,6,24-26} Furthermore, the 422-symmetry model for the octamer according to Timasheff and Townend⁵⁸ possesses a large central cavity which could accommodate trapped water; if the NMR experiment observed this trapped water, the τ_c value found would be less than that of the protein. Also, if the assumption is made that the NMR hydration of the octamer itself at 2°C equals $(\bar{v}'_w)_{\text{pH}4.65} - (\bar{v}'_w)_{6.2}$, values from 0.019 to 0.028 g H₂O per gram protein can be calculated by the three methods described above. The total volume of the cavity, approximated by an internal sphere tangent to the subunits on the basis of known structural parameters,⁵⁸ amounts to about 6.5 nm³. Taking the specific volume of water as unity and thus its molecular volume as 0.03 nm³ per molecule, this would correspond to about 220 moles H₂O per mole of octamer, or 0.027 g H₂O per gram protein, which is within range of the NMR-derived hydration values for the octamer.

Since the derived NMR correlation times are number-average values, the hypothesis that the increase in hydration accompanying octamer formation is largely due to trapped water may be tested by calculating a number-average correlation time from the relationship $(\bar{v}'_w)_{4.65} \tau_c = (\bar{v}'_w)_{6.2} (\tau_c)_0 + [(\bar{v}'_w)_{4.65} - (\bar{v}'_w)_{6.2}] (\tau_c)_{\text{cc}}$, where $(\tau_c)_0$ is the correlation time of the octamer at 2°C (i.e., 145 ns, see Table 1), $(\tau_c)_{\text{cc}}$ is the correlation time of the central cavity of volume 6.5 nm³ (i.e., 1.4 ns), and $(\bar{v}'_w)_{6.2}$ and $(\bar{v}'_w)_{4.65}$ are the NMR hydration values at pH 6.2 and 4.65, respectively. Calculation of τ_c from ^2H NMR hydration values by method I at 2°C gives 36 ns, in fair agreement with the ^2H NMR experimental value of 32.2 ± 4.6 ns at pH 4.65 and 2°C. While the results of this calculation furnish an indication of the reasonableness of the approach, they do not, however, show any exact mechanism of increased hydration accompanying octamer formation.

In contrast to method I, method II assumes no constant quadrupole coupling constant and therefore may serve, incidentally, to calculate values of e^2qQ/\hbar (assuming $\eta = 0$) from the \bar{v}'_w values and the relaxation increments obtained by deuterium NMR, together with the experimentally derived τ_c . The quadrupole coupling constants calculated for the respective methods range from 120 to 160 kHz. Hunt and MacKay³⁹ have correlated O...²H...O and N...²H...O hydrogen-bond distances with values of quadrupole coupling constants. From their relationships and the above e^2qQ/\hbar values, one obtains distances for O...²H...O from 0.15 to 0.17 nm, and for N...²H...O from 0.16 to 0.20 nm. These compare with linear hydrogen bond lengths of 0.181 to

0.187 nm recently reported by Ceccarelli et al.⁶³ in an extensive review of neutron diffraction data.

c. Contrast of NMR Hydration with Preferential Hydration

To contrast these NMR hydration results with results from another physical method which measures water-protein interactions, preferential hydrations were obtained by Wyman's theory of linked functions,^{10,64} from which it follows that for a tetramerization reaction (dimer \rightarrow octamer, in the case of β -LgA)

$$\begin{aligned} d\ln K_T / d\ln a_{X,T} &= (\bar{v}_{X,T})_{\text{pref}} - 4(\bar{v}_{X,M})_{\text{pref}} \\ &= -(W_T/X_T)[(\bar{v}_{W,T})_{\text{pref}} - 4(\bar{v}_{W,M})_{\text{pref}}] \end{aligned} \quad (19)$$

where the preferential interactions are defined by

$$(\bar{v}_X)_{\text{pref}} = \bar{v}_X - \left(\frac{X}{W}\right) \bar{v}_W \quad \text{and} \quad (\bar{v}_X)_{\text{pref}} = \bar{v}_X - \left(\frac{W}{X}\right) \bar{v}_X \quad (19a)$$

Here K_T is the association constant, a_X is the activity of salt, $(\bar{v}_{X,T})_{\text{pref}}$ and $(\bar{v}_{X,M})_{\text{pref}}$ are the preferential salt binding of octamer (subscript T) and dimer (subscript M), and $(\bar{v}_{W,T})_{\text{pref}}$ and $(\bar{v}_{W,M})_{\text{pref}}$ are the preferential hydrations, respectively. Preferential interaction parameters can thus be readily obtained from the slope of a plot of association constants at various salt concentrations vs. the activity of the salt at the corresponding concentrations.

Association constants can be calculated by the use of Gilbert's theory for rapidly reequilibrating association in a sedimenting boundary.^{65,66} Gilbert has shown that for a reversible association there exists a minimum concentration, c_{min} , above which bimodality of a schlieren ultracentrifuge pattern appears. Furthermore, the area of the slow peak remains constant as the loading concentration is increased well above c_{min} , which is related to the equilibrium constant of the association. Thus, for a tetramerization (in this case, dimer \rightarrow octamer),⁴⁸⁻⁵⁰

$$K_T = M_M^3 \delta [1 + \delta/4(1 - \delta)]^3 / [16(1 - \delta)c^3] \quad (20)$$

where $\delta \equiv (s - s_1)/(s_2 - s_1)$, (s , s_1 , and s_2 being the sedimentation coefficients for the leading edge of the boundary, for the dimer, and for the octamer, respectively), K_T is the association constant, c is the total loading concentration, and M_m is the dimer molecular weight. Since $\delta_{\text{min}} = (n - 2)/3(m - 1)$ and $\delta = 2/9$ for $n = 4$ (where n is the degree of association), $K_T = 1.087 \times 10^{12}/c_{\text{min}}^3$. The product of the percentage of the slow peak and the loading concentration equals c_{min} , and K_T can thus be evaluated.

In this way, sedimentation velocity data for β -Lg A at pH 4.65 give a linked-function plot (Figure 5B), which clearly shows a negative slope. From the least-squares value of this slope, a preferential solvation of -3.78 moles salt per mole octamer is calculated. With the assumption that the tetramerization does not release any salt, a value of 0.258 g H_2O per gram protein for the preferential hydration is obtained, presumed to be equal to $(\bar{v}'_w)_{\text{pH}4.65} - (\bar{v}'_w)_{\text{pH}6.2}$ from NMR at 2°C . The linked-function preferential hydration thus appears to differ significantly from the NMR hydration difference.

However, as previously noted, NMR probably samples only a certain percentage of the total hydration of a protein. For example, if a major portion of the bound water has a τ_c value of less than 1 ns, its contributions to the spin-lattice and spin-spin relaxations of the bound state would be equal since at 9.17 MHz the T_1/T_2 ratio for this fast-tumbling water would be unity. Therefore, the correlation time and hydration values calculated from the NMR results by use of a two-state

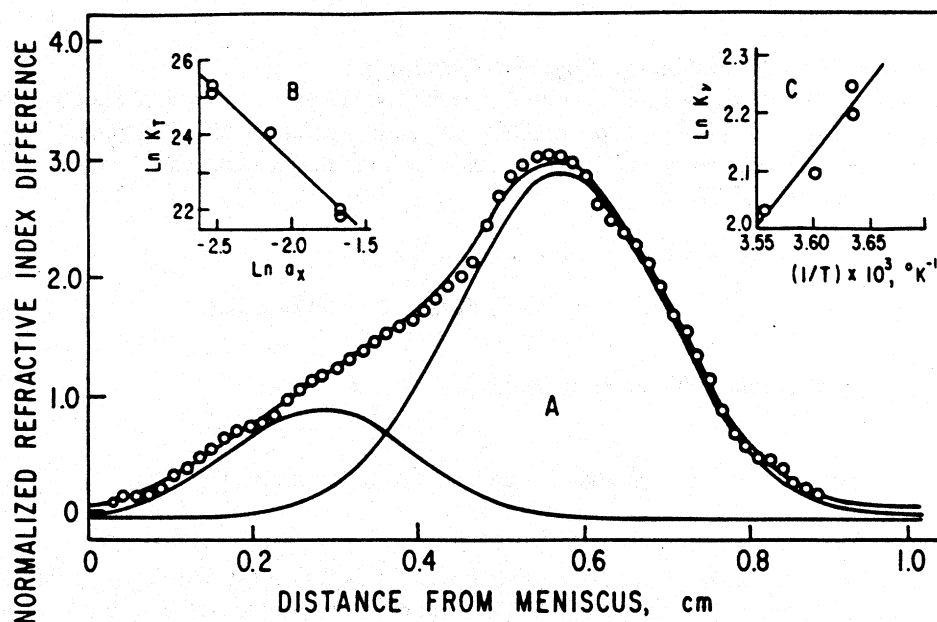


FIGURE 5. (A) Sedimentation of β -Lg A under association conditions. Gilbert pattern (open circles) and decomposition into two Gaussian peaks (solid lines). (B) Linked-function plot. Plot of logarithm of tetramerization equilibrium constant vs. logarithm of activity of salt. The slope is a measure of preferential hydration. (C) van't Hoff plot. Plot of logarithm of equilibrium constant of water binding vs. reciprocal of absolute temperature. The slope gives a value -5.5 ± 1.2 kcal for the enthalpy of hydration. (From Kumosinski, T. F. and Pessen, H., *Arch. Biochem. Biophys.*, 218, 286, 1982.)

model approximation would yield number-average values weighted toward the slow-tumbling component. It would probably be more realistic to compare the enthalpies of hydration derived by NMR with those from linked functions by the van't Hoff relationship (Figure 5C). This is possible by assuming a thermodynamic model involving the transfer of free water to bound water as protein is added to the solution, i.e., $\Delta G = RT \ln (\bar{v}_w/55.6)$. Values of ΔG , ΔH , and ΔS of hydration for each of the three NMR methods are shown in Tables 2 and 3.

From the slope of the van't Hoff plot of Figure 5C, a ΔH of -5.5 ± 1.2 kcal/mol dimer is obtained. ΔS values calculated at each temperature average -14.1 ± 0.03 e.u. The small SD for ΔS indicates constancy of the entropy with respect to temperature and lends support to the model. Furthermore, ΔH of hydration values from NMR range from approximately -6 to -9 kcal/mol dimer, seemingly in agreement, within experimental error, with the value of -5.5 derived from linked functions. Nevertheless, it needs to be remembered that the linked-function method measures the difference between the total hydrations of octamer and dimer, whereas the NMR method yields a quantity proportional to the total hydration of the octamer. Direct comparison of the temperature dependence of these two methods, by assuming that the linked-function hydration is proportional to the difference in the NMR hydration at pH 4.65 and 6.2, is not feasible since the proportionality constant itself should change as a function of temperature. However, the total hydration of the dimer appears to be temperature independent, as indicated by essentially constant NMR hydration values at pH 6.2 for 30 and 2°C. These considerations lead to an alternative evaluation of the NMR data in terms of a three-state model.

i. Isotropic Binding, Three-State Model

For the reasons indicated, an attempt was made to evaluate the ^2H NMR relaxation increment on the basis of a three-state model (i.e., free water, fast- and slow-tumbling bound water), as used

Table 4
TOTAL HYDRATION FOR β -LACTOGLOBULIN DERIVED FROM
A THREE-STATE MODEL ($^2\text{H NMR}$)^{a,b}

pH	T (°C)	$(\bar{v}'_w)_f$	$(\bar{v}'_w)_s$	$(\tau_c)_s$ (ns)	$-(\Delta H)_s$ (kcal)
6.2	30	0.1	0.0054 ± 0.0008	11.0 ± 2.7	0
	2	0.1	0.0056 ± 0.0020	33.9 ± 4.1	
4.65	30	0.201	0.0085 ± 0.0002	28.8 ± 3.3	6.0 ± 1.6
	2	0.358	0.0235 ± 0.0003	42.3 ± 4.6	

^a Assumptions: $(\tau_c)_f = 48$ ps; $(R_{1b})_f = (R_{2b})_f = 31.94$ s⁻¹ at 30°C for pH 6.2 and 4.65; $(R_{1b})_f = (R_{2b})_f = 70.27$ s⁻¹ at 2°C for pH 6.2 and 4.65. Subscripts f and s refer to fast-tumbling and slow-tumbling fractions, respectively.

^b Adapted from Reference 27.

by Cooke and Kuntz in treating lysozyme data,⁶⁷ with the following assumptions. First, the fast-tumbling hydration component of dimer was assumed to be 0.1 g water/per gram protein on the following grounds. The lysozyme crystal has been determined to contain 80 molecules of water per protein molecule, or 0.1 g H₂O per gram protein,⁶⁸ and 100 to 300 water molecules per crystalline protein molecule distributed over the molecular surface have generally been reported.⁶⁷ For β -Lg, 200 moles water per mole protein is equivalent to 0.1 g water per gram protein. Also, Teller et al.⁶⁹ have shown that experimentally derived frictional coefficients from sedimentation results are in agreement with those calculated from known X-ray crystallographic structures provided water molecules are added to each charged side chain on the protein surface. The β -Lg dimer has 90 charged amino acids;⁷⁰ a value of 0.1 g water per gram protein corresponds, therefore, to about two water molecules bound to each charged side-chain amino acid.

Second, since from Teller's work, this water would be bound to charged side chains, and since Brown and Pfeffer⁷¹ have shown that deuterium-modified lysine groups tumble at 48 ps, a τ_c value of 48 ps can be assumed. Any water bound to lysine should then have a τ_c value no lower than that of the side chain itself. It was assumed also that, because of the fast segmental motion of the side chain, any increase in association of the protein would not affect this τ_c unless the side chain was directly involved in the interaction site. However, the viscosity and temperature effect on the Stokes-Einstein relationship was taken into account when the temperature changes from 30 to 2°C. Finally, the fast-tumbling hydration values at pH 4.65 were increased, by 0.101 (30°C) and 0.258 (2°C) g H₂O per gram protein, respectively, in line with the linked-function results, which indicate such preferential hydrations at these temperatures.

Subtraction of the fast-tumbling contribution from the $^2\text{H NMR}$ spin-lattice and spin-spin relaxation increments yields new values from which the correlation time of the slow component, $(\tau_c)_s$, and its corresponding hydration, $(\bar{v}'_w)_s$, can be calculated. Table 4 shows that the $(\tau_c)_s$ are slightly larger than the τ_c of Table 1, and the $(\bar{v}'_w)_s$ are slightly larger than the \bar{v}'_w of Table 2 for the two-state model. However, the corresponding values are probably within experimental error, as are the derived enthalpy of hydration of the slow component (Table 4) and the enthalpy of hydration derived from the two-state model (Table 2). Calculation of a number-average correlation time of the slow component of the octamer, by assuming that the increase in

hydration upon octamer formation is due to water trapped in the cavity of the octamer, yields 37 ns. This is in reasonable agreement with the experimentally derived value of (τ_c) at pH 4.65 and 2°C of 42.3 ± 4.6 ns (Table 4).

ii. Anisotropic Binding Mechanism

The preceding calculations assume an isotropic relaxation mechanism, as detailed above. In the presence of salt, all the relaxation at pH 6.2 can be accounted for by a slow-tumbling and a fast-tumbling component, amounting to 13 and 204 mol H₂O per mole dimer, respectively, and increasing at pH 4.65 and 2°C to 61 and 730 mol H₂O per mole dimer; these may be considered reasonable values for the hydration of a protein.^{1,72}

This does not, however, eliminate the possibility of an anisotropic relaxation mechanism for hydrodynamically bound water. The present results may be interpreted equally well on the basis of the three-component derivation in conjunction with either a two- or three-state model and an appropriate order parameter $S < 1$ (see Equations 16c and d). Here a three-state model is defined, as for the isotropic mechanism (Table 4), as comprising free-motion water, a slow-motion component (i.e., $\tau_c > 5$ ns), and a fast-motion component (i.e., $\tau_c \cong 48$ ps, as assumed in Table 4). For the latter, under extreme-narrowing conditions the factor S^2 attached to Equations 16c and d is changed to $(1 - S^2)$.⁷ The slow motion, in either the two- or three-state anisotropic mechanism, may be due to such processes as protein reorientation, internal motion of the protein, or translational diffusion of water along the protein surface.^{7,34}

Reported values of $S = 0.06$ from ¹⁷O relaxation⁷ have been derived by applying to a protein the line-splitting data obtained for a liquid crystal, on the assumption that three to six water molecules are bound to carboxyl groups and one to three to hydroxyl groups. Theoretical results of Walmsley and Shporer³⁴ give relationships for S (termed the scaling factor by these authors) based on ¹H, ²H, and ¹⁷O relaxation. From these it follows that a value of $S = 0.06$ for ¹⁷O would imply $S = 0.12$ for ²H. At pH 6.2 (30 and 2°C) and pH 4.65 (30 and 2°C) one obtains (from Equations 13a to c and the ²H NMR data of Table 1 for the two-state, and those of Table 4 for the three-state model) hydrations, all in units of g H₂O per gram protein, of 0.483, 0.500, 0.660, and 2.090 for the two-state, and 0.298, 0.295, 0.509, and 1.250 for the three-state model, respectively. A more reasonable estimate is obtained from the theoretical relationships of Walmsley and Shporer, together with the experimental results of Koenig et al.,^{5,6,24} which give $S = 0.23$ and corresponding hydrations, in the same units, of 0.119, 0.136, 0.180, 0.569, and 0.102, 0.105, 0.163, 0.435. The ΔH of hydration at pH 4.65 is found to be -6.8 for the two-state and -5.9 kcal for the three-state model. These results agree with the isotropic mechanism (Tables 2 and 4), since S enters simply as a factor in the Kubo-Tomita-Solomon equations.

Alternatively, equating the preferential hydration from linked functions with the difference between the 2°C ²H NMR hydrations at pH 4.65 and pH 6.2, one obtains $S = 0.30$ for the two-state and $S = 0.26$ for the three-state model, both not far from the 0.23 predicted from the theory of Walmsley and Shporer. Furthermore, with the above values of S , the pH 4.65 enthalpies of hydration are -6.8 and -5.9 kcal for the two- and three-state models, respectively. Thus, the increase in hydration as well as the corresponding enthalpy change attendant on octamer formation are the same for either assumption of relaxation mechanism.

B. Influence of Protein Hydrophobic and Electrostatic Self Association: Bovine Casein

From the previous section, it appears that hydrophilic self-association of proteins can increase hydration values through changes in quaternary structure. An extension of this work would be to study the influence of protein-protein interactions involving hydrophobic and electrostatic groups on the hydration of proteins as evaluated by NMR relaxation measurements. The model system chosen was casein, a family of phosphoproteins which are the major components of milk.^{73,74} Casein monomers undergo hydrophobic self-associations at pH 7 which increase with increasing temperature.^{75,76} The associated state is commonly referred to as the submicellar form.^{75,77} Upon addition of calcium, casein polymers further associate via

calcium phosphate salt bridges into a colloidal state referred to as the micellar form.^{73,77} Although the chemical and physical properties of the individual caseins are well documented, few studies have addressed the association properties of the whole complex as found in milk. For these reasons, NMR relaxation measurements of water were made with varying concentrations and temperatures of casein under both submicellar and micellar conditions.⁷⁸

1. Experimental Procedures

a. Preparation of Solutions

Casein micelles were isolated from 2 l of fresh warm milk to which 1 g of phenylmethyl sulfonyl fluoride had been added to retard proteolysis. The milk was centrifuged at $4000 \times g$ for 10 min to remove the cream fraction; 400 ml of this skim milk was centrifuged for 1 h at $88,000 \times g$ (37°C). The pellets were washed twice in D_2O containing 25 mM piperazine-*N,N'*-bis(2-ethanesulfonic acid) (PIPES) (pH 6.75), 20 mM CaCl_2 , and 80 mM KCl. The final protein concentration was fixed at about 100 mg/ml (total volume of 5 ml). Subsequent dilutions were made with the same buffer. To produce submicelles, sodium caseinate prepared from the same skim milk was dialyzed and lyophilized at pH 7.2; the lyophilized protein was dissolved in D_2O , in the same PIPES-KCl buffer without CaCl_2 , but with added dithiothreitol to promote self-association of κ -casein.⁷⁶ These procedures were designed to minimize the concentration of H_2O in the D_2O solutions and thus to eliminate any significant contribution to the relaxation rates from deuterium exchange. Casein concentrations were determined spectrophotometrically on samples diluted 1/50 to 1/100 in 0.1 *N* NaOH; an absorptivity of $0.850 \text{ ml}\cdot\text{mg}^{-1}\cdot\text{cm}^{-1}$ at 280 nm was used for whole casein.⁷⁶

b. Relaxation Measurements

Measurements were made essentially as described under β -Lg A above, except that only deuteron resonance relaxation was investigated at 9.17 MHz, on samples at pH 7.0, at 2, 15, and $30 \pm 1^\circ\text{C}$. These rates were measured in D_2O to avoid cross-relaxation effects between water and protein protons, such as have been observed by Edzes and Samulski³⁶ and by Koenig et al.⁵⁴

2. Analysis of Data

a. General Considerations

Bovine casein is composed of four major proteins, α_1 -, α_2 -, β -, and κ -casein, in the approximate ratios of 4:1:4:1.⁷⁹ α_1 -casein contains 8 phosphoserines; β -casein contains 5 phosphoserines; κ -casein contains on the average 1 phosphoserine, while α_2 is variable, containing 8 to 11.⁷⁴ All caseins are generally considered to have little or no ordered secondary structure and to contain a large number of hydrophobic residues. With the above assumptions, the average molecular weight of monomeric casein is estimated to be 23,300; the average partial specific volume, \bar{v} , is 0.736 ml/g; and the weight-average number of phosphate groups is 6.6 per 23,300-Da monomer unit.

At pH 6.75 with no calcium present, studies of the individual caseins have shown that they undergo mainly hydrophobically driven self-associations which increase with increasing temperature and ionic strength.⁷⁷ Studies on whole casein are limited but show similar results.^{76,77} Figure 6A shows one proposed structure of this limiting polymer, commonly referred to as the submicellar form of casein. Here, the hydrophobic core is considered to be composed mostly of the hydrophobic portions of α_1 - and β -caseins, while κ -casein resides mostly at the surface because of its ability to keep α_1 - and β -caseins from precipitating at 37°C in the presence of calcium. All charged groups, including the serine phosphates, are located on the surface of the submicellar structure. In this model, the κ -casein content of the submicelles is variable.

Upon addition of calcium, these submicellar spherical particles are thought to self-associate by way of calcium phosphate salt bridges to form a large colloidal spherical particle of approximate radius of 65 nm, called the micellar form of casein (see Figure 6B). The integrity

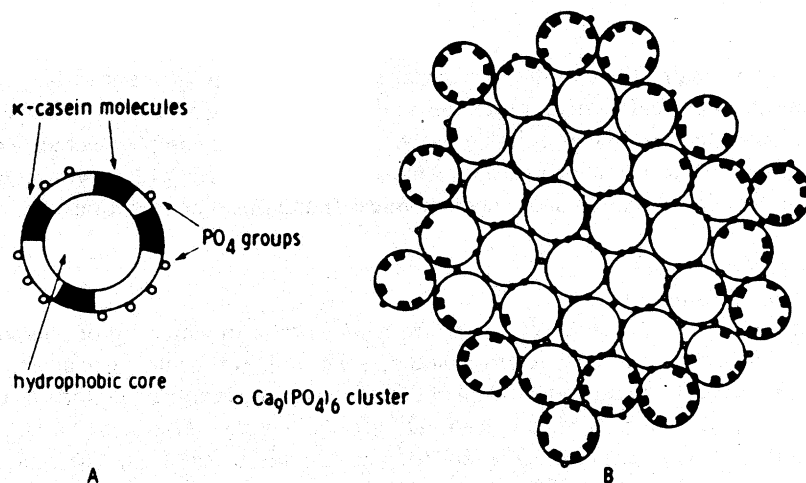


FIGURE 6. Quaternary structural forms of casein. A. submicellar form and B. micellar form upon addition of calcium. (From Schmidt, D. G., *Developments in Dairy Chemistry*, Vol. 1, Fox, P. E., Ed., Applied Science, Essex, England, 1982. With permission.)

of the submicelle is thought to be preserved upon the addition of calcium if enough calcium is used and no phosphate buffer is present to compete with the serine phosphate interaction sites. Moreover, it has been conjectured by several investigators that trapped water exists within the micellar structure.¹ The characteristic of κ -casein to be present predominantly on the surface of the micelle has been shown by electron microscopy coupled with gold-labeled κ -casein,⁷⁷ or with ferritin conjugate and anti- κ -casein.⁸⁰

For the above reasons, ²H NMR relaxation measurements, both spin-lattice, R_1 , and spin-spin, R_2 , of D₂O with varying concentrations of casein were made on casein, with and without calcium, at 30, 15, and 2°C. Figure 7 shows R_1 and R_2 measurements at 15°C under submicellar and micellar conditions. All data were fitted by Equation 13a, modified by replacing the concentration, c , by the protein activity, a_p , with $a_p = c \exp(2B_0 c + \dots)$, where B_0 is the second virial coefficient of the protein. Least-square fits were obtained by means of a Gauss-Newton nonlinear regression program. The experimental data and the data calculated from the model employed are in excellent agreement, as shown by the solid line in Figure 7. Under these and all other conditions investigated, the nonlinear portion of the curves yielded a virial coefficient of 0.0032 ± 0.0003 ml/mg, indicating the consistency of the experimental results. The linear portions of the curves were evaluated with a propagated SE of about 4%; they contain the product of the relaxation of the bound water, hydration, and finally the asymmetry parameter, S . These parameters are separated and each is discussed in the following section.

b. Hydration and Dynamics: Isotropic Model

From the linear portion of spin-lattice and spin-spin relaxation results, Equation 13a, and the Kubo-Tomita-Solomon equations, Equations 16a and b, the following parameters were calculated at the various environmental conditions of the caseins: correlation times, τ_c , hydration values, \bar{v}_w , for an isotropic tumbling model ($S = 1$), and the relaxation rates of the bound water, R_{1b} and R_{2b} . The results are shown in Table 5. Here, \bar{v}_w values increased from 0.00652 to 0.01201 g water per gram protein and τ_c values decreased from 38.9 to 29.8 ns as the temperature decreased from 30 to 2°C for casein in the submicellar form; propagated standard errors were about 8% for τ_c and 6% for \bar{v}_w . The same temperature dependence of τ_c and \bar{v}_w was exhibited under micellar conditions, although at all temperatures their absolute values were larger for the micellar than for the submicellar form.

At this point it may be noted that although the caseins are self-associating, one needs to consider here only the aggregated form. The concentrations used were high enough so that the

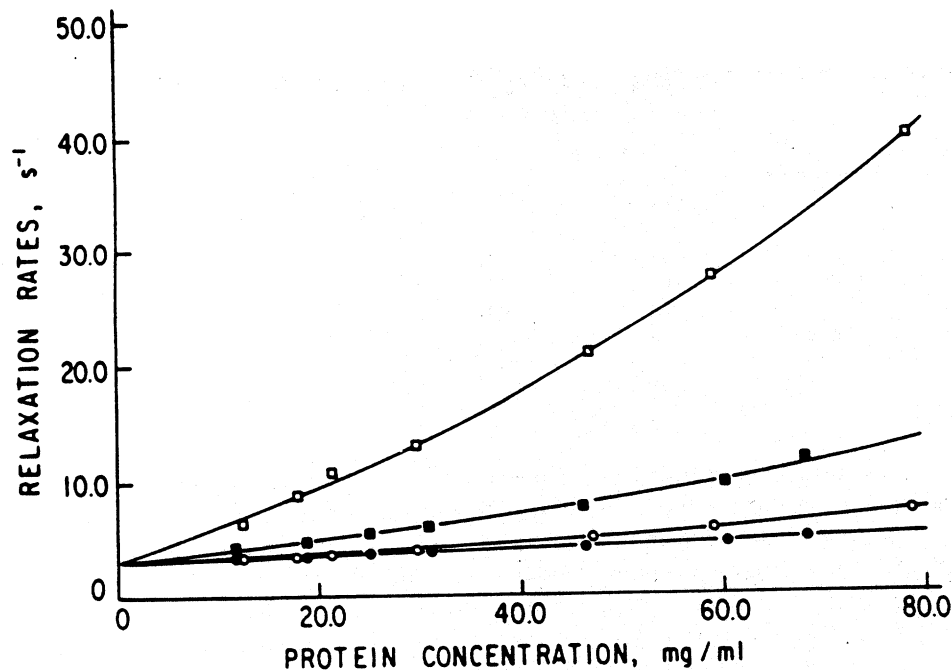


FIGURE 7. Dependence of deuteron relaxation rates of water on casein concentrations in D_2O at pH 6.75 in 0.2 M PIPES-KCl buffer at 15°C. \bullet - \bullet -. R_2 measurements, submicellar form; \square - \square -. R_2 measurements, submicellar form; and \circ - \circ -. R_2 measurements, micellar form; \square - \square -. R_2 measurements, micellar form. (From Reference 78.)

Table 5
HYDRATION AND DYNAMICS OF BOUND WATER FOR CASEINS

	Temperature (°C)	τ_c (ns)	\bar{v}_w (g H ₂ O per gram protein)	R_1 (s ⁻¹)	R_2 (s ⁻¹)
Submicelle	30	38.9	0.00652	1904	10.510
	15	34.7	0.00824	2080	9.840
	2	29.8	0.01201	2323	9.070
Micelle	30	63.6	0.0165	1249	14.790
	15	51.1	0.0225	1515	12.570
	2	45.1	0.0282	1689	11.530

association equilibrium favors polymer formation.^{75,77} For both micelles and submicelles, no significant differences in hydration would result from protein concentration-dependent dissociation effects at 30°C. (At lower temperatures, this must be qualified as discussed further on.) Also, these \bar{v}_w values will in most probability show only a fraction of the total hydration, since at 9.17 MHz any bound water with $\tau_c < 6$ ns would have an R_2/R_1 ratio of unity and would not be observable by this methodology.

Since it had been shown previously that the τ_c values derived from NMR relaxation results are those for the unhydrated rather than the hydrated form of the protein,^{27,81} the Stokes radius, r , calculated from τ_c values using the Stokes-Einstein relationship would indeed be a representation of the quaternary structure for the unhydrated protein. Such r values were calculated for the caseins from all τ_c results and are listed in Table 6.

A Stokes radius of 3.64 nm (Table 6) found at 30°C is at the lower limit of radii reported for

Table 6
MOLECULAR PARAMETERS OF CASEINS DERIVED FROM DATA OF
TABLE 5

	Temperature (°C)	r (nm)	M _p	(v _w) _c	S	(v _w) _c = 0.237
Submicelle	30	3.64	165.000			0.116
	15	3.05	97.200			0.147
	2	2.55	56.800			0.214
Micelle	30	4.29	270.700	0.469	0.188	0.294
	15	3.48	144.500	0.357	0.251	0.400
	2	2.93	86.200	0.380	0.272	0.502

submicelles, whose sizes range from 4 to 9 nm depending on the method of measurement.^{76,77,82,83} (It should be recalled that direct comparison between Stokes radii derived by this NMR method and those calculated from hydrodynamic or small-angle scattering data would be inappropriate since these latter include water of hydration, whereas the NMR values pertain to the anhydrous protein.^{27,81}) Results for the submicelles show a decrease in hydration value (Table 5) and an increase in Stokes radius (Table 6) with increasing temperature. This suggests that hydrophobic interactions are involved in the formation of the submicelle, since, as the temperature is raised, water is excluded from the hydrophobic interface during an association process.

Although the absolute value of the Stokes radius calculated for the micelle was on the same order of magnitude as that of the submicelle, it was not as large as might expected, evidently because of experimental limitations. These limitations are due to the large size of the casein micelle (r = 65 nm), which would result in a τ_c value of nearly 200 μs. Such a slow motion would yield a spin-relaxation rate too large to be seen by these NMR experiments at 9.17 MHz. In one sense, what the data may show is the average hydration of the caseins within the micelle, since the fastest motions dominate relaxation data. The micelle exhibits the same temperature dependence as the submicelle, showing hydrophobic interactions, in agreement also with earlier investigators who theorize that micelles are formed by aggregation, via Ca²⁺ salt bridges, of submicelles.^{73,77} The slight increase in r from submicelle to micelle is probably due to a gradual increase in internal hydration (trapped water) as the submicelle is incorporated into the micelle. In the course of micelle formation, the electrostatic forces involving Ca²⁺ and phosphate or carboxyl groups on the exterior of the submicelle are in competition with, and finally outweigh, the hydrophobic effects within the submicelle.

c. Derived Molecular Parameters of the Protein

Since it has been shown that the Stokes radius of the bound water derived from NMR relaxation results can be related to the anhydrous volume,^{27,81} a molecular weight of the caseins can be calculated from

$$M_p = 4/3 \pi r^3 N_A / \bar{v}_p \quad (21)$$

where r is the Stokes radius (Table 6), N_A is Avogadro's number, and \bar{v}_p is the average partial specific volume of the caseins, taken here to be 0.736. The results are shown in Table 6. Here the increase in M_p for both the submicelle and the micelle, as the temperature is increased, is a qualitative indication of hydrophobic self-association not only for the submicelle, but also within the micelle structure itself.

To quantitate this temperature-dependent variation of M_p, apparent equilibrium constants K_A were calculated from K_A = M_p/23,300, where 23,300 is the average monomer molecular weight of casein. (This relationship is reasonable since the measurements were performed at high

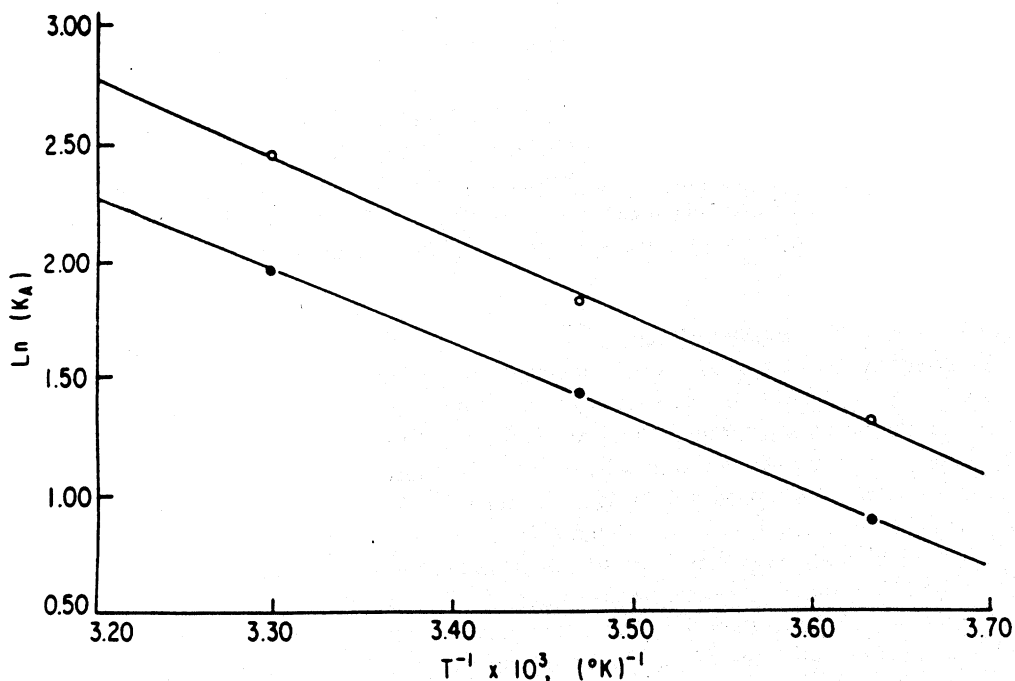


FIGURE 8. van't Hoff plots for temperature dependence of the self-association of casein. ●-●-, submicellar form and ○-○-, micellar form. (From Reference 78.)

concentrations of casein, where the equilibrium is driven nearly completely toward the aggregated form.) The $\ln K_A$ and the inverse temperature ($1/T$) were then used with the van't Hoff expression (see Figure 8) to calculate the apparent enthalpy of self-association, ΔH , for submicellar and micellar casein. As can be seen in Figure 8, the van't Hoff plots for the two forms of casein are essentially parallel. In fact, ΔH values for the submicelle formation were 6.34 ± 0.11 kcal. and for the self-association to the micelle only slightly higher at 6.81 ± 0.28 kcal. These values are in good agreement with ΔH of 4.67 found for the association of purified α_1 - and κ -caseins.⁸⁴ This quantitation of the temperature variation of the self-association strongly suggests that the integrity of the submicelle is at least partly preserved when it is incorporated into the micellar form by Ca-phosphate salt bridges. Moreover, extrapolation of the van't Hoff plot to 37°C yields an apparent molecular weight of 210,000 which is in agreement with results from other investigations.^{77,82,85}

Finally, an average charge Z per average monomer molecular weight $M_p = 23,300$ can be evaluated from the virial coefficient B_0 of 0.0032 ml/mg using the following expression:⁸⁶

$$2 B_0 = \frac{Z^2}{4m_s M_p} + \bar{v}_p/1000 \quad (22)$$

where m_s is the molarity of salt used. The value of ± 8.1 , calculated from the NMR relaxation measurements, is not in good agreement with the average value of -16.1 , which was derived from the amino acid sequence,⁷⁴ average pK values from the literature, and the assumption that at pH 6.75, where these experiments were performed, the serine phosphates have a charge of -2 . However, Arakawa and Timasheff⁸⁷ have shown that another term must be added to Equation 9, to take into account the preferential interactions of salt and water at the protein interface, namely the quantity $-(\partial g_s/\partial g_p)^2/m_s$, where $(\partial g_s/\partial g_p)$ is the preferential binding term. If this is

added to Equation 9, with Z chosen as -16.1 , and $B_0 = 0.0032$ ml/mg, a value of 0.046 g salt per gram protein is found for the preferential binding term. For micellar casein this value is reasonable, if one translates Ca^{2+} binding of 0.043 g salt per gram protein into 8.5 mol Ca^{2+} per mole of $23,300$ -Da protein. This is consistent with the notion of Ca^{2+} binding to phosphate groups since, as stated above, the weight-average value for all the caseins is 6.6 phosphates per monomer.

d. Hydration: Anisotropic Tumbling Model

Up to this point, all hydration values were calculated using an isotropic motion mechanism of the bound water ($S = 1$). However, the motion of the bound water may in fact be anisotropic ($S < 1$) if the correlation times are long with respect to the Larmor frequency. Such may be the case for the casein micelles where water may be trapped at the surfaces of submicelles as they self-associate via calcium-phosphate salt bridges into micelles. In the following, an attempt, although speculative in nature, is made to calculate the asymmetry factor S for casein.

In Table 6, r values at all temperatures are somewhat larger for the micellar form of casein than for the submicellar form. This consistently larger Stokes radius (also represented by the molecular weight, M_p , in Table 6) could be due to increased hydration either by weakening of hydrophobic interactions within the submicellar form, caused by calcium phosphate salt bridge formation, or to trapped water at the surfaces of the submicelles as they are incorporated into the micelle. This increased hydration value, $(\bar{v}_w)_r$, may easily be calculated from the Stokes radii of the micelle, r_m , and submicelle, r_{sm} , by

$$(\bar{v}_w)_r = \bar{v}_p \left(\frac{4/3 \pi r_m^3}{4/3 \pi r_{sm}^3} - 1 \right) \quad (23)$$

where $\bar{v}_p = 0.736$ for an average partial specific volume of the caseins. The results, shown in Table 6, range between 0.357 and 0.469 g water per gram protein at these temperatures. Asymmetry values, S , can now be calculated from $S = (\bar{v}_w / (\bar{v}_w)_r)^{1/2}$ and the \bar{v}_w and $(\bar{v}_w)_r$ values from Tables 5 and 6, respectively. These S values are listed in Table 6 and average 0.237 ± 0.033 , in good agreement with the value of 0.23 predicted by Walmsley and Shporer.³⁴ New hydrations $(\bar{v}_w)_{S=0.237}$ can now be calculated for an anisotropic motion mechanism using the \bar{v}_w values of Table 5 and the average S of 0.237 . These are listed in the last column of Table 6. The absolute values of these new hydrations, ranging from 0.116 to 0.502 g water per gram protein for submicellar and micellar casein, are closer to the expected hydration values derived by other methods.^{27,81}

It should be stressed that, although the above calculation is not proof of the existence of water with anisotropic motion bound to casein, it does furnish valuable information. What is important here is the variation of hydration with quaternary structural changes of the casein rather than its absolute value. It may be that the absolute value of the hydration derived from NMR relaxation results will be obtained only some time in the future when the controversy regarding the isotropic vs. anisotropic nature of water binding to proteins in solution is resolved. At any rate, water bound at the surface of the micelles or influenced by the slow motion of the large particle would not be sensed at the frequencies used in these studies.

Here it has been found that the hydration value, no matter what absolute value is used, decreases and that r increases with increasing temperature for submicellar casein, in agreement with the general notion of hydrophobic protein self-association. Moreover, this same temperature-dependent variation of \bar{v}_w and r exists for micellar casein, indicating preservation of the submicelle structure within the micelle. The consistent increase in r and \bar{v}_w for the micellar form over the submicellar form clearly demonstrates that trapped water exists in the micellar form of casein, as had been predicted by Kuntz and Kauzmann.¹

IV. CROSS RELAXATION

A. Influence of Environmental Changes on β -Lactoglobulins

Much controversy exists in the literature concerning the use of proton NMR relaxation rates for measuring the hydration of proteins. In fact, there has been little unanimity on this subject because of the complex nature of hydration phenomena and their relationships to NMR relaxation, and because of complicating factors such as cross relaxation between protein and water protons. Examination of water-protein interactions by measurement of proton spin relaxation of water in a well-defined system of a protein capable of undergoing structural changes should, however, afford opportunity to observe correlations between these changes and the measured relaxations.

A suitable protein for this purpose is β -lactoglobulin, which occurs in two genetic variants, A and B, possessing physical properties nearly identical except for the extents of specific structural changes.^{50,51,58,88-91} Pessen et al.⁸ have reported measurements of the longitudinal (R_1) and transverse (R_2) proton relaxation rates of water in buffered solutions as a function of protein concentration, with pH and temperature varied to allow examination of several of the protein structural states for concomitant differential behavior between the two variants. These data were evaluated first in terms of very simple model assumptions for the water-macromolecule interaction, with the aim of determining (1) whether significant changes in this interaction can be found for dilute solutions of this model protein as a result of environmental changes and (2) whether such changes can be shown to reflect the respective molecular states of the protein, as reported in the literature from studies by other methods under the same conditions. Next, the consequences of considering cross relaxation were examined. As a special alternative to such other methods as those using magnetic field dependence of NMR relaxation^{24,92} or measurements on solvent ^{17}O and ^2H nuclei,^{24,27,54} the combined use of proton NMR data from the two genetic variants was explored, making use of their differing association behavior. The results of cross relaxation evaluated in this way can be compared with the previous results from ^2H NMR relaxation as well as with other protein structural information obtained from hydrodynamics, X-ray diffraction and small angle X-ray scattering.

1. Experimental Procedures

a. Preparation of Solutions

β -Lactoglobulins A and B (β -Lg A, β -Lg B) were the recrystallized lyophilized products, prepared from the milk of homozygous A/A and B/B cows by the method of Aschaffenburg and Drewry.⁹³ To exclude the possibility that observations might be affected by paramagnetic enhancement due to the presence of heavy-metal ions, some experiments were carried out both with and without prior treatment of the preparations with EDTA. In no case was a significant difference found. Distilled water from an all-glass still was used without further treatment. The buffers employed were pH 4.65, 0.1 M acetate (β -Lg B) and 0.3 M acetate (β -Lg A); pH 6.2, 0.1 M phosphate (β -Lg A) and 0.1 M acetate (β -Lg B); pH 8.0, 0.1 M glycylglycine plus 0.1 M KCl, adjusted to pH by addition of KOH. All buffer salts were the potassium salts of the respective acids and were Baker Analyzed reagents. Glycylglycine was purchased from Calbiochem, and benzene- d_6 and acetone- d_6 (99.5 atom %) were purchased from Wilmad Glass Co., Inc.

Protein solutions, prepared 1 d before use, were exhaustively dialyzed overnight against buffer at 0 to 5°C, except for the study at pH 8.0. In that case, all manipulations, including filling of the sample cells, were carried out at room temperature, and the low-temperature measurements were made last. All dilutions were made with the appropriate dialyzate. Protein concentrations were determined using an absorption coefficient of 0.96 ml·mg⁻¹·cm⁻¹ at 278 nm.¹⁷

b. Relaxation Measurements

Measurements were made essentially as described under β -Lg A above, except that spectra

were obtained from two different spectrometers (R_1 measurements, at 90 MHz, from a Bruker WH-90; R_2 measurements, at 59.79 MHz, from a JEOL FX60Q), at 2° and $30 \pm 1^\circ\text{C}$. To avoid exceeding the dynamic range of the computer with consequent signal truncation, it was necessary to provide the Bruker WH-90 with a 20-db attenuator in the probe preamplifier, in addition to reducing the sample volume for both instruments by the use of a microcell assembly with an expendable 35- μl sample bulb (Wilmad Glass Co., Inc.). The assembly included this microbulb, filled with the sample and inserted into either a 10- or 5-mm OD sample tube containing deuterated solvent (benzene- d_6 or acetone- d_6) to provide an external heteronuclear lock signal.

2. Analysis of Data

a. Relaxation Increments and Free-Water Relaxation Rates

In the following, it will be convenient to supplement the notation of Equations 13 a to c by the introduction of a few modified quantities. Letting $h \equiv \bar{v}_w$, (in grams bound water per gram dry protein) and $\Delta R \equiv R_b - R_f$ (i.e., the difference in relaxation rates of protein-influenced and free states of water, or the total excess relaxation rate), it is noted from Equations 13a and 13b that the relaxation increment, $(dR_{\text{obs}}/dc)\mu = k$, becomes identical to the specific excess relaxation rate, $(R_{\text{obs}} - R_f)/c$, if the concentration dependence of R_{obs} is linear. Furthermore, the quantity $h \Delta R$, termed the hydration product, equals these other two quantities only in the absence of cross relaxation; i.e., k is a hydration product uncorrected for cross relaxation effects. The appropriate correction is made in conjunction with the topic of cross relaxation below. (The R and k terms throughout may be subscripted with 1 or 2, depending on whether they pertain to longitudinal or transverse relaxation.)

Typical concentration dependences for R_1 and R_2 data are shown in Figures 9A and 9B, respectively, and are seen to be linear, in agreement with the original theory. Values of k_1 and R_{1r} , and of k_2 and R_{2r} , calculated by linear regression of the respective dependence of relaxation rates on protein concentration (Equation 13c), are listed in Table 7. As expected,⁶⁰ the relaxation rates of bulk water protons, R_{1r} and R_{2r} , increased at the lower temperature in each of these systems; the magnitude of the change did not differ significantly among the solvent buffers used. The relaxation increments k_1 and k_2 also changed in the same direction.

Values of k_1 , k_2 , R_{1r} , and R_{2r} so found were used, as described, in the calculation of apparent degrees of hydration h , uncorrected for cross relaxation (also listed in Table 7), as well as apparent rotational correlation times and longitudinal and transverse relaxation times for water in the bound state, R_{1b} and R_{2b} (not listed). In each case, R_{2b} increased while R_{1b} decreased at the lower temperature. This temperature effect is consistent with the absence of an exchange contribution, as is implicit in Equations 16a and b.⁹⁴

b. Structural States and Hydration

The temperatures at which measurements were made had been chosen because of known properties of the protein. At both pH 4.65 and 8.0, it is known to undergo significant structural changes, mainly in the cold; at pH 6.2, no change in structure accompanies the same temperature change. On inspection of the temperature and pH dependence of the various parameters in Table 7, it is noticeable that not only h but also the hydration product k_2 appears to be suitable as at least a preliminary measure of hydration: allowing for the temperature effect (exhibited by itself at pH 6.2), k_2 and h on going from 30 to 2°C at pH 4.65 display increases by factors of 2.7 and 3.1 for the A variant and of 2.3 and 2.5 for the B variant, while at pH 8.0, the A variant shows increases by factors of 1.7 for k_2 and 2.0 for h . These indications of pronounced increases in apparent hydration in the cold at both pH 4.65 and 8.0 may be interpreted in terms of the known molecular behavior of β -Lg.

This protein has been reported to occur naturally in five genetic variants.⁷⁴ The A and B forms employed here undergo a variety of changes in conformation and state of association, summarized in Figure 10. The investigation described here focused on two of these: a slow, irreversible

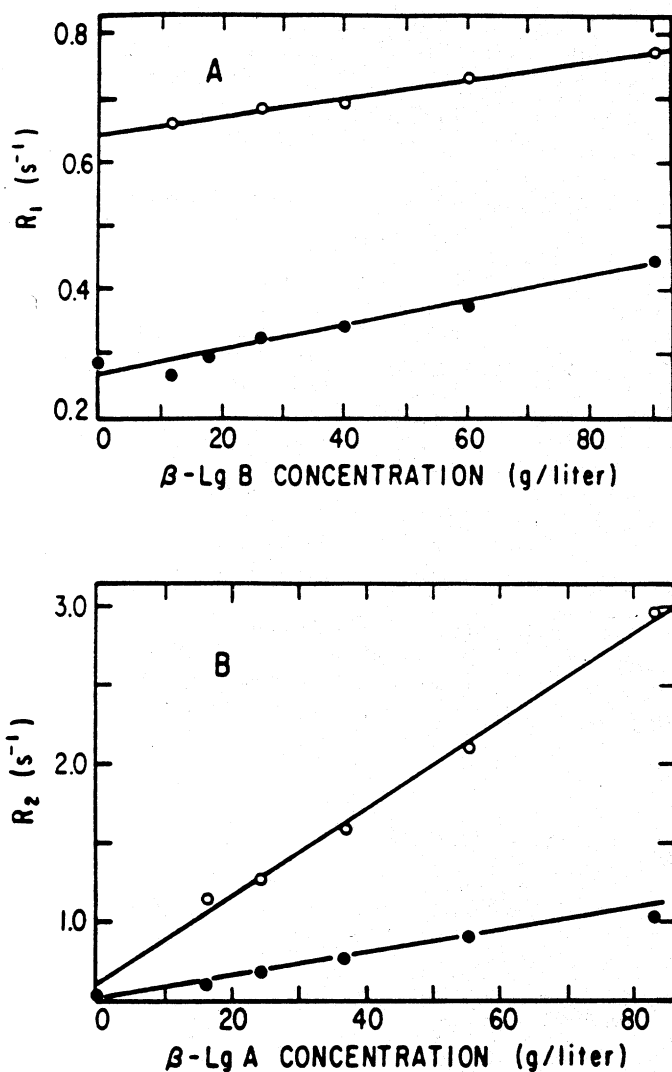


FIGURE 9. Proton relaxation rates of water in β -Lg solutions as a function of protein concentration. The slope (k) is the relaxation increment, and the intercept (R_f) is the relaxation rate of free water, as described in Section III. A.2. (A) Proton longitudinal relaxation rates (R_1) of water as function of β -Lg B concentration at pH 6.2. Temperatures: (-●-●-), 30°C ($k_1 = 1.94 \pm 0.18$, $R_{1f} = 0.271 \pm 0.009$) and (-○-○-), 2°C ($k_1 = 1.49 \pm 0.11$, $R_{1f} = 0.643 \pm 0.006$). (B) Proton transverse relaxation rates (R_2) of water as function of β -Lg A concentration at pH 8.0. Temperatures: (-●-●-), 30°C ($k_2 = 7.0 \pm 0.2$, $R_{2f} = 0.53 \pm 0.01$) and (-○-○-), 2°C ($k_2 = 27.9 \pm 1.3$, $R_{2f} = 0.61 \pm 0.06$). (From Reference 8.)

denaturation⁹¹ and a rapid dimer \rightleftharpoons octamer equilibrium,^{50,51,58,89,90} both occurring primarily in the cold. The 2-subunit, 36,700-Da dimer is the kinetic unit persisting over a wide range of moderate conditions of pH from 3 to about 7,⁸⁹ its structure has been reported in detail.^{95,96}

Above pH 6.5, the dimer is known to begin to dissociate^{97,99} and then to denature irreversibly^{98,100,101} while at first remaining in solution. This time-dependent denaturation, referred to as "cold-denaturation" since it is accelerated in the cold as compared to room temperature, occurs about three times faster with β -Lg A than with β -Lg B.⁹¹ This correlates well with the observed indication of increased hydration of β -Lg A on exposure to the cold, since both the concurrent

Table 7
RELAXATION INCREMENTS (LONGITUDINAL, K_1 , AND TRANSVERSE, K_2)
AND SOLVENT RELAXATION RATES (R_{1r} AND R_{2r}) FOR SOLUTIONS OF TWO
VARIANTS OF β -LACTOGLOBULIN^a

pH	Variant	Temp. (°C)	Relaxation increment ($s^{-1} \cdot g_{\text{water}} \cdot g^{-1}_{\text{prot}}$)		Solvent relaxation rate (s^{-1})		Uncorrected hydration ($g_{\text{water}} \cdot g^{-1}_{\text{prot}}$) <i>h</i>
			k_1	k_2	R_{1r}	R_{2r}	
4.65	A	30	1.52 ± 0.25	8.9 ± 1.5	0.307 ± 0.011	0.23 ± 0.07	0.070 ± 0.012
		2	3.56 ± 0.23	55.3 ± 4.4	0.603 ± 0.010	0.70 ± 0.24	0.298 ± 0.021
4.65	B	30	1.26 ± 0.26	5.2 ± 0.4	0.314 ± 0.004	0.34 ± 0.02	0.047 ± 0.008
		2	2.18 ± 0.24	27.7 ± 2.6	0.644 ± 0.011	0.60 ± 0.16	0.163 ± 0.017
6.2	A	30	1.92 ± 0.26	4.5 ± 0.2	0.301 ± 0.007	—	0.056 ± 0.005
		2	—	10.4 ± 1.2	—	0.89 ± 0.06	0.077 ± 0.007
6.2	B	30	1.94 ± 0.18	—	0.271 ± 0.009	—	—
		2	1.49 ± 0.11	—	0.643 ± 0.006	—	—
8.0	A	30	1.77 ± 0.13	7.0 ± 0.2	0.264 ± 0.005	0.53 ± 0.01	0.064 ± 0.004
		2	2.73 ± 0.51	27.9 ± 1.3	0.514 ± 0.015	0.61 ± 0.06	0.178 ± 0.023

^a Longitudinal measurements (at 90.0 MHz) and transverse measurements (at 59.79 MHz), made at two temperatures and three values of pH, as indicated. Values of the parameters are the results of linear least-square fits to points at five to seven concentrations, each representing the mean of \pm quadruplicate relaxation rate determinations based on measurements at five time values each. Error terms indicate standard errors of the parameter.

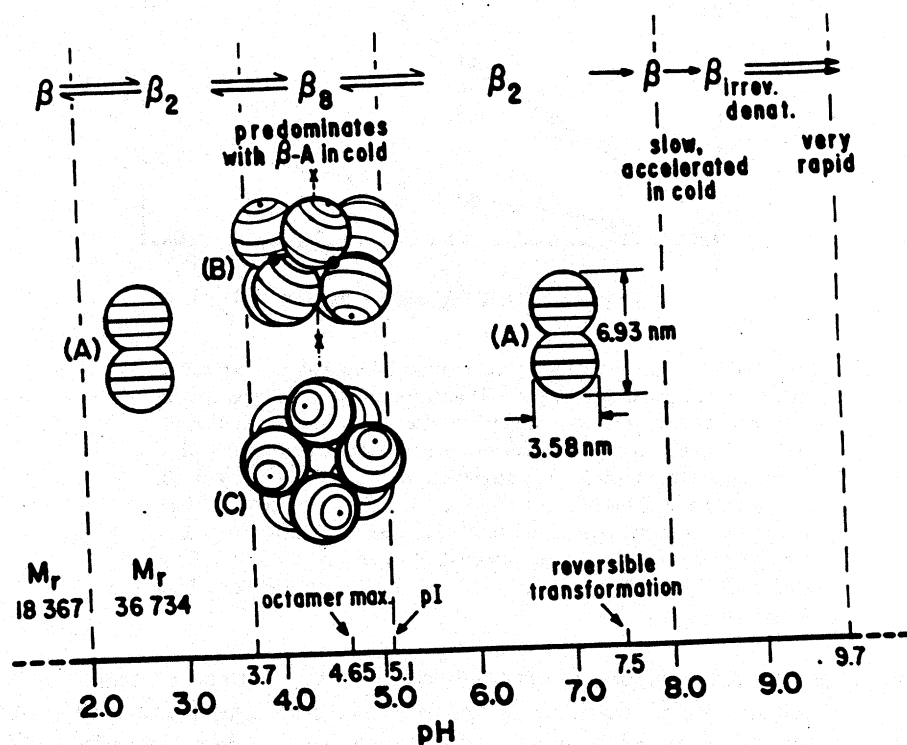


FIGURE 10. Schematic representation of changes in the structure of β -lactoglobulins as a function of pH. β : β -lactoglobulin. Insets (molecular models): (A), dimer; (B), octamer, with square decahedral faces on top and bottom; O, octamer bonds; X-X, tetrad axis; circular lines indicate monomer equators and parallels perpendicular to the dimer axes; and (C), octamer, with square faces in front and back, tetrad axis perpendicular to plane of paper. (Adapted from Reference 8. Based on data of References 50, 51, 58, 88 to 91, 95 to 101, and 108.)

dissociation and subsequent denaturation presumably involve increased availability of water-binding sites on the denatured protein molecule.

Between pH 3.7 and 5.1, self-association of β -Lg dimer to octamer occurs as temperature decreases. This is a rapid equilibrium process that is also well characterized;⁵⁰ it occurs to a greater extent with the A variant than with the others. Since self-association involves protein-protein interactions which should remove some of the potential water-binding sites on the dimer surface, a decrease in hydration might be expected. The observed increased hydration requires a more detailed examination of the molecular geometry. The octamer, as determined by Timasheff and Townend,⁵⁴ is a closed ring, consisting of four dimers associated symmetrically about a tetrad axis; its general shape is that of a decahedron with a substantial central cavity (Figure 10, insets B and C). Because of a sizable hole (approximately 1.4 nm diameter) in each of the two square faces of the decahedron (Figure 10, inset C), the water in the interior of the octamer is readily accessible for fast exchange with the bulk water on the outside, as was assumed by the theory above.

An estimate of the amount of water contained in the cavity may be obtained from the geometric parameters,⁵⁸ which indicate that an inscribed sphere, tangent to the interior van der Waals surfaces of the octamer, would have a volume of about 6.45 nm³. (This estimate neglects the spaces in corners and crevices of the cavity; these will be largely offset by the dimer-dimer contact areas between the eight monomer units, which tetramerization makes unavailable to water binding at the 12 new protein-protein contact sites.) From the molecular weight and volume of water and the molecular weight of the protein,⁵⁶ one finds that this cavity corresponds to 0.0264 g H₂O per gram protein. It can, therefore, accommodate a considerable amount of water detectable by NMR, giving rise to the increased hydration observed under the conditions where octamer formation occurs. It may now also be seen that the relative enhancements of the hydration parameters noted above (i.e., factors of 3.1 for h and 2.7 for k_2 for the A variant vs. 2.5 and 2.3, respectively, for the B variant) are consistent with the known higher degree of octamer formation by β -Lg A compared with B.⁵⁰

There is, thus, qualitative agreement between the hydrations shown in Table 7 and the known structure of the corresponding states of the protein, but it remains to be examined how this agreement may be affected by a consideration of cross relaxation.

c. Dynamics and Hydration from Transverse Relaxation

Values of apparent correlation times calculated from Equations 5b, 6, and 7 range from 1.4 to 7.1 ns, considerably lower than corresponding estimates obtained for β -Lg from the Debye-Einstein relation⁶⁰ for dielectric relaxation (15 to 53 ns¹⁰²) or fluorescence depolarization (20 to 78 ns⁶²), or from NMR by means of a method which obviates the effects of cross relaxation (10 to 32 ns²⁷). The lowered apparent correlation times may be considered a clear indication of cross relaxation,³³ not clearly evidenced here in the form of nonexponential relaxation only because of the vast excess of bulk water protons in dilute solutions. Instead, it shows its presence by its effect on the apparent τ_c and by increasing the apparent water proton relaxation rate, R_1 ,^{53,103} and, thus, the values of k_1 . These, as well as the validity of the uncorrected Equation 13c, require further examination, especially as there is definite evidence for the general occurrence of cross relaxation in protein systems.^{36,53,54,103}

Since, however, cross relaxation affects primarily longitudinal relaxation,^{36,54} one may start by dealing separately with the transverse relaxation, for which Equation 13c will continue to serve in conjunction now with the added information supplied by the availability of data for both genetic variants at pH 4.65. For this purpose, the extent of tetramerization for each variant at this pH at 2°C can be calculated from light-scattering data of Kumosinski and Timasheff⁵⁰ as 91.2% (β -Lg A) and 31.0% (β -Lg B).

This information allows the values of k_2 from Table 7 to be expressed in terms of the relative contributions of dimer and octamer and, together with the knowledge of the amount of water in

the cavity and Equation 13c, provides two simultaneous equations for the two variants. In this way, a number of parameters of interest not affected by cross relaxation can be obtained (Appendix, a). These include the hydrations of dimer, $h_D = 0.0276$ g/g, and octamer, $h_O = 0.0540$ g/g, various correlation times, and the Stokes radius of the octamer, $R_{s,O} = 3.82$ nm. Repetition of this calculation for 30°C with the separately determined values of k_2 of Table 7 at that temperature, combined with the information⁵⁰ that the extents of tetramerization here are 26.9% (β -Lg A) and <0.02% (β -Lg B), gives $h_D = 0.0223$ g/g, $h_O = 0.0487$ g/g, and $R_{s,O} = 3.75$ nm. The values of $R_{s,O}$ from measurements at the two temperatures thus are in close agreement, as would be expected since the Stokes radius should be nearly temperature independent. They are in general agreement also with literature values of 4.33 nm, from sedimentation;⁶¹ 4.44 nm, from small-angle X-ray scattering;^{48,61} and 3.04 nm, from ²H NMR.²⁷

d. Cross Relaxation and Longitudinal Relaxation

Longitudinal relaxation data can be utilized in similar manner when Equation 13c is modified by decomposition into a corrected term, $k'_1 \equiv h' \Delta R$ (where h' is a hydration corrected for cross relaxation), and a term for a cross-relaxation increment, k_x , to account for the contribution of cross relaxation to k_1 . The justification for such a procedure derives from a consideration of a cross-relaxation model which treats the water and protein protons as separate thermodynamic systems in magnetic interaction^{54,74} (Appendix, b). This results in values at 2°C (see Appendix, c) for the k_1 terms for octamer and dimer, respectively, of $k_{x,O} = 3.71$ and $k_{x,D} = 1.39$. Since spin diffusion, which is the basis for cross relaxation, should be dependent on distance from particle center of mass to surface (see Reference 54), the pertinent distance for the fairly isotropic octamer should be approximately its Stokes radius, 4.33 nm,⁶¹ whereas for the dimer, consisting of two tangent, nearly spherical monomer subunits, it should be approximately the monomer radius, 1.79 nm.⁵⁸ The ratio of these distances is 2.42, while the ratio $k_{x,O}/k_{x,D} = 3.71/1.39$ is 2.67, and thus in good agreement with the value estimated from the known geometry. (The 30°C values, based on k_1 values and extents of tetramerization much smaller, and, therefore, containing larger relative errors, yield a ratio $k_{x,O}/k_{x,D} = 1.86$, which, however, is still of the correct order of magnitude.)

To examine the phenomena at pH 8.0, a first assumption was made that k_x at 30°C may be approximated by its value for the dimer at pH 4.65, at the opposite side of the isoelectric point of 5.1, since additional cross relaxation due to higher pH should be largely offset by decreased spin diffusion with the here more disordered protein. For pH 4.65, the modified Equation 5b, $k_1 = h_D \Delta R_1 + k_x$, with $h_D = 0.0223$ obtained from k_2 , and with the k_1 of Table 7, gives $k_x = 1.088$. This value, substituted in the same equation applied to the pH 8.0 conditions, gives $h_D \Delta R_1 = 0.69$ and, from Equation 6, $\tau_c = 5.36$ ns, or a Stokes radius of 1.88 nm. Compared to the approximately 1.79 nm Stokes radius of the monomer,⁵⁸ this implies that at this alkaline pH, even at room temperature, a substantial fraction of the protein exists as monomer. This is in agreement with the findings of Townend et al.⁹⁷ and Georges et al.,⁹⁸ according to which the dimer at room temperature above about pH 7.0 begins to dissociate before alkaline denaturation takes place. Since this might weaken the above assumption regarding k_x , one may look, alternatively, to the pH 6.2, 2°C data for confirmation. Used as before, these yield a k_x of 1.43 which, applied to the pH 8.0, 2°C data, gives $\tau_c = 8.67$ ns, or a Stokes radius of 1.68 nm, and again the distinct indication is of a prevalence of monomer, in accord with the literature.

Cross-relaxation increments and hydrations calculated in this manner for the various forms of the protein under the different conditions, as well as the respective correlation times and Stokes radii, are listed in Table 8 (where h' designates values obtained by taking cross relaxation explicitly into account; see Appendix, b). Correlation times here range from 10.2 to 51.2 ns, more in keeping with the literature values cited above.^{27,62,102} In view of the various approximations made and the high contribution of k_x to k_1 , the values of h' listed must, however, be considered to be somewhat less accurate than their standard errors would indicate.

Table 8
**PARAMETERS CALCULATED FOR β -LACTOGLOBULIN SOLUTIONS WITH CROSS RELAXATION
 TAKEN INTO ACCOUNT^a**

pH	Variant or species	Temp (°C)	k_a (s ⁻¹ · g _{water} ⁻¹ · g ⁻¹ prot)	h' (g _{water} ⁻¹ · g ⁻¹ prot)	τ (ns)	R_{NMR} (nm)	
						This work Literature	
4.65	A	30	1.34 ± 0.25	0.029 ± 0.001	12.5 ± 1.5		
		2	3.50 ± 0.23	0.052 ± 0.009	51.2 ± 4.6		
	B	30	1.09 ± 0.26	0.022 ± 0.002	10.2 ± 0.1		
		2	2.11 ± 0.24	0.036 ± 0.008	33.0 ± 1.6		
	Pure dimer	30	(1.09 ± 0.26) ^b	(0.022 ± 0.002) ^b	10.2 ± 0.1		
		2	1.39 ± 0.32	0.028 ± 0.010	23.6 ± 0.1		
Pure octamer	30		0.049 ± 0.002	18.6 ± 5.6	3.75	4.33 ^d , 4.44 ^e , 3.04 ^f	
	2	3.71 ± 0.25	0.054 ± 0.010	(42.2 ± 12.4) ^g	3.82		
6.2	A or B	30	2.03 ± 1.29 ^h		53.8 ± 5.0		
		2	1.79 ± 0.18		(102.6 ± 38.4) ^h		
8.0	A	30	3.52 ± 0.19	0.019 ± 0.001	10.2 ± 0.1		
		2	1.09 ± 0.26	0.021 ± 0.002	23.6 ± 0.1		
	Pure octamer	30	2.08 ± 0.51	0.047 ± 0.009	5.4 ± 0.3	1.88 ^d	1.79 ^g
		2		0.103 ± 0.007	12.4 ± 0.6	1.68 ^e	

^a Based on data of Table 7 and Equations 16 and 29. For statistics, see legend to Table 7.

^b Pure octamer without cavity contribution.

^c Parameters of B variant.

^d From cross relaxation at pH 4.65.

^e From cross relaxation at pH 6.2.

^f From Reference 61.

^g From Reference 61, as calculated from Reference 48.

^h From Reference 27.

ⁱ From Reference 58.

The contributions of cross relaxation indicated by k_c (Table 8) comprise the major parts of the values of k_1 (Table 7): for either variant, under all three pH conditions, k_c at 30°C amounts to about 90% of k_1 . This could be expected, inasmuch as solutions of proteins ranging in molecular weight from 30,000 to 100,000, under various conditions of concentration and temperature, have been found to exhibit zero-field cross relaxation rates already roughly equal to water proton relaxation rates.⁵⁴ At higher frequencies, the ratio of cross relaxation to total proton relaxation must increase further, since cross relaxation, particularly for proteins of molecular weight above 20,000 and at resonant frequencies near 100 MHz, increases substantially with frequency,^{53,104} while the bound-water proton relaxation rate decreases (see Equation 16a). This expectation should hold for the present data relating to a 37,000-Da protein examined at 90 MHz. It is notable, however, that k_c at 2°C, which for pH 4.65 and 6.2 amounts to more than 97% of k_1 , for pH 8.0 shows a marked drop to 76%, in agreement with the predicted loss of spin diffusion in the more disordered state under these denaturation conditions.

e. Significance of Parameters

In regard to the significance of the hydration parameter h , it is well recognized^{1,29,94} that any technique used to measure hydration of proteins implies an operational definition of the water observed as "bound" that pertains to that particular technique, as well as to the model used to analyze the data thus obtained. The results described here pertain to rotationally as well as irrotationally bound water,¹⁵ together with the effects of inter- as well as intramolecular contributions to relaxation. Cross relaxation effects have already been mentioned. Anisotropic surface effects also may well play a role, as dealt with by Walmsley and Shporer³⁴ and Halle et al.⁷

Using the approach of these authors, one can relate the hydration values shown in Table 8 to hydrodynamic hydration values in the literature by taking into account the effects of the anisotropic surface environment of the protein molecule. This involves the use of a scaling factor³⁴ or order parameter S ,⁷ which is nearly independent of the specific protein, and which enters Equations 16a and b so as to change the R_b value by a factor of S^2 , and consequently h (related to R_b by Equation 13c) by very nearly $1/S^2$. From the data of Koenig et al.,⁶ and the arguments of Walmsley and Shporer³⁴ as embodied in Figure 3 of these authors, one obtains an estimate of S as approximately 0.21. Applying this, as indicated, to the values of h' of Table 8 gives conventional hydrations from 0.43 to 0.50 for the pH 4.65 and 6.2 dimer at room temperature. This is squarely within the 0.30 to 0.54 range, clustering around 0.46, reported for β -Lg in the literature.¹

Without the use of S , the h' values of Table 8, ranging from 0.019 for dimer at 30°C, pH 6.2, to 0.052 for the A variant at 2°C, pH 4.65, may be directly compared with results from a method based on deuterium NMR to avoid the effects of cross relaxation, which gave corresponding values from 0.015 to 0.043 (Table 3 of Reference 27).

While the hydration values of Table 8 are smaller than the uncorrected ones of Table 7 (roughly half, or less), in either set the relationships between them under the various conditions are not greatly different. It is seen, therefore, that no matter in which way one prefers to interpret the data of Table 7, one can obtain definite correlations with known structural information, and that, contrary to doubts expressed in the literature,^{24,54} relaxation measurements at the frequencies employed here contain considerable structural information relating to the solute protein. Furthermore, because one should be concerned mainly with changes rather than absolute values of h , other effects not specifically evaluated may largely cancel. Although absolute values obtained for a hydration parameter may be very dependent on model assumption, observed changes in such a parameter are less dependent on assumptions and can be equally useful in correlations with structural changes.

Returning to the questions posed at the outset, one sees that it is possible by a simple procedure to obtain useful hydration parameters which can account, at least in a qualitative

fashion, for the effects of (1) cold-denaturation of β -lactoglobulin A at alkaline pH and (2) of octamer formation of β -lactoglobulin at pH 4.65; (3) give a quantitative account of the effect on relaxation of the marked difference between variants A and B in octamer formation; (4) provide quantitative cross relaxation information; and (5) confirm such conjectures as that of Beall et al.¹⁰⁵ regarding correlation of water proton relaxation rate changes with changes in molecular states of a protein. It thus indicates that observed proton relaxation rate changes can be used by way of the parameter h or h' to evaluate concurrent structural changes in a given system.

3. Appendix

a. Parameters from Transverse Relaxation Increments and Solvent Relaxation Rates

Summing the contributions to k_2 of dimer and octamer for each variant according to Equation 13c, one has, from Table 7, the two simultaneous equations

$$k_{2,A} = 55.3 = 0.912 h_o \Delta R_{2,o} + (1 - 0.912) h_D \Delta R_{2,D} \quad (24a)$$

and

$$k_{2,B} = 27.7 = 0.310 h_o \Delta R_{2,o} + (1 - 0.310) h_D \Delta R_{2,D} \quad (24b)$$

where h_o , the hydration of the octamer, is that of the dimer, h_D , augmented by the contribution of the cavity i.e., $h_o = h_D + 0.0264$; and where $\Delta R_{2,o}$ and $\Delta R_{2,D}$ are the total excess transverse relaxation rates for octamer and dimer, respectively. $R_{2,D}$ can be obtained by way of an estimate of the correlation time of the dimer, τ_D , from the known dry volume of the latter, suitably corrected for its deviation from spherical shape.

The Einstein diffusion equation, expressing the rotary diffusion coefficient D_{rot} in terms of spherical volume V , provides a correlation time equal to $V\eta/kT$,⁶⁰ where k is Boltzmann's constant, 1.381×10^{-16} erg/ $^\circ$ K, and η is the viscosity of solvent, approximated sufficiently by that of water, 0.01673 and 0.00801 P at temperatures T of 275.2 and 303.2 $^\circ$ K, respectively. V equals vM/N_A , where v , the partial specific volume of β -Lg, is 0.751 ml/g,¹⁰⁶ M is $2 \times 18,370$, and N_A is Avogadro's number, 6.022×10^{23} mol $^{-1}$. The correlation times for spheres then would be 20.18 ns at 2 $^\circ$ C and 8.77 ns at 30 $^\circ$ C. Application of the shape factor 1.168 for the elongated β -Lg dimer⁶² gives values for τ_D of 23.57 ns at 2 $^\circ$ C and 10.24 ns at 30 $^\circ$ C; from Equation 24, together with the values of R_{2f} from Table 7, $\Delta R_{2,D}$ becomes 488.6 s $^{-1}$ at 2 $^\circ$ C and 231.8 s $^{-1}$ at 30 $^\circ$ C.

Equations 8a and b can now be solved for the remaining unknowns, which are found to be $h_D = 0.0276$ and $\Delta R_{2,o} = 1096.8$. It follows that $h_o = 0.0276 + 0.264 = 0.0540$. From $\Delta R_{2,o}$ and R_{2f} at 2 $^\circ$ C from Table 7, one obtains $R_{2b,o}$ and, by means of Equation 16b, the correlation time $\tau_{o,h}$ of the hydrated octamer, 53.82 ns. The latter may be regarded as the sum of weighted correlation times of dry octamer, τ_o , and the cavity water, $\tau_{cav} = V_{cav}\eta/kT$. With the values of V_{cav} and η above, τ_{cav} equals 2.839 at 2 $^\circ$ C and 1.234 ns at 30 $^\circ$ C. Thus, at 2 $^\circ$ C, $53.82 = (0.0276/0.0540)\tau_o + (0.0264/0.0540)(2.839)$, and $\tau_o = 102.6$ ns. However, from $\tau_o = V\eta/kT = 4\pi R_{s,o}^3/3kT$, where $R_{s,o}$ is the Stokes radius of the octamer, follows $R_{s,o} = 3.82$ nm.

b. Cross-Relaxation Increment

The cross-relaxation model results in a set of simultaneous differential equations for the coupled magnetization decays of water and protein protons in terms of: corresponding reduced magnetizations, $M_w(t)$ and $M_p(t)$, defined as $M(t) \equiv (A_- - A_+)/2A_-$ (see Equation 17); corresponding longitudinal relaxation rates in the absence of cross relaxation, R_w and R_p ; the rate of magnetization transfer from water to protein protons, R_{τ} ; and the ratio of water to protein protons, n_w/n_p . Standard methods lead to a double-exponential solution of the form^{23,36,54}

$$M_{w,p}(t) = C_{w,p}^+ \exp(-R^+t) + C_{w,p}^- \exp(-R^-t) \quad (25)$$

where R^+ and R^- refer to two apparent relaxation rates, fast and slow respectively, which are the same for both kinds of proton and are given by

$$2R^\pm = R_p + R_w + R_T n_w/n_p + R_T \pm [(R_p - R_w + R_T n_w/n_p - R_T)^2 + 4R_T^2 n_w/n_p]^{1/2} \quad (26)$$

Judging from the data of Koenig et al.,⁵⁴ where neglecting the $4R_T^2 n_w/n_p$ term in Equation 26 in comparison with the terms preceding it resulted in less than 5% error, one may approximate the component rates of the double-exponential relaxation by

$$R^+ \approx R_p + R_T n_w/n_p \quad \text{and} \quad R^- \approx R_w = R_T \quad (26a)$$

In dilute solutions, $n_w \gg n_p$, and R^+ becomes so large that the first right-hand term of Equation 25 is small compared to the second term. (This, together with a pulse-width dependence, was the reason why the double exponential was not detectable in graphs of the original data.) The observed relaxation rate then becomes $R \approx R_w + R_T$ and, since the observed proton longitudinal relaxation can be expressed as the sum of contributions from the two states as well as from cross relaxation,

$$R_{\text{obs}} = p_b R_b + p_f R_f + R_T \quad (27)$$

Here p_b and p_f are the fractions of protons in the respective state, so that $p_b = hc$, and $p_f = 1 - p_b = 1 - hc$.

Since for dilute solutions R_T should be proportional to the protein concentration c , or $R_T k_x c$, Equations 13b and c can be rewritten as

$$R_{\text{obs}} = R_f + [(h' \Delta R) + k_x]c = R_f + (k_1 + k_x)c \quad (28)$$

where

$$k_1 = h' \Delta R, \quad k_x = k_1 + k_x \quad (28a)$$

and the observed relaxation increment now equals the sum of the hydration product and the cross relaxation increment. The term k_x , it should be noted, is an approximate representation of R_T , reflecting in addition the combined effects of the simplifying assumptions made above.

c. Parameters from Longitudinal Relaxation Increments and Solvent Relaxation Rates

In analogy to Equations 24a and b, one has

$$k_{1,A} = 3.56 = (0.912)(0.0540)\Delta R_{1,O} + (1 - 0.912)(0.0276)\Delta R_{1,D} + k_{x,A} \quad (29a)$$

and

$$k_{1,B} = 2.18 = (0.310)(0.0540)\Delta R_{1,O} + (1 - 0.310)(0.0276)\Delta R_{1,D} + k_{x,B} \quad (29b)$$

Here, $\Delta R_{1,O}$ and $\Delta R_{1,D}$ are found from Equation 13a with $\tau_{O,n} = 53.82$ and $\tau_{D,n} = 23.57$ ns, together with the appropriate R_{1f} from Table 7, as 0.969 and 2.936/s⁻¹, respectively. With these values, $k_{x,A} = 3.50$ and $k_{x,B} = 2.11$. Considering each of these, in turn, to be made up of contributions from octamer, $k_{x,O}$, and dimer, $k_{x,D}$, one has the two equations

$$k_{x,a} = (0.912)k_{x,O} + (1.088)k_{x,D} \quad (30a)$$

and

$$k_{x,b} = (0.310)k_{x,O} + (0.690)k_{x,D} \quad (30b)$$

which yield $k_{x,O} = 3.71$ and $k_{x,D} = 1.39$.

B. Overview

To relate resonance relaxation behavior to protein structural states, pulse Fourier transform NMR was employed to obtain water proton longitudinal and transverse relaxation rates (R_1 and $R_{1\rho} = R_2$) of bovine β -Lgs A and B in buffered solutions. Measurements at concentrations from 5 to 100 mg/ml were made at pH 4.65, 6.2, and 8.0, at 30° and 2°C, to monitor specific structural changes. The parameters characterizing the concentration dependence of the observed R_1 and R_2 were used to derive a number of quantities relating to protein-influenced water, including a hydration parameter h . Changes in h under the different sets of conditions were correlated with (1) the irreversible denaturation of this protein at pH 8.0, 2°C and (2) the dimer \rightleftharpoons octamer association at pH 4.65, 2°C. Corresponding correlation times, however, were low, indicating cross relaxation which had not manifested itself as nonexponential relaxation because of the large amount of water present. Differences in the extent of the dimer octamer association between genetic variants A and B allowed an evaluation of dynamics and extent of hydration from R_2 alone, assuming the absence of intermolecular interactions. Derived parameters were in agreement with hydrodynamic and X-ray values in the literature. Cross relaxation was likewise evaluated and was found to contribute to R_1 to a large extent. The results show that changes in proton relaxation rates in solutions of a globular protein occurring as genetic variants with different physical properties (such as β -Lg) can be utilized to detect variations in hydration corresponding to changes in molecular association and conformation, as well as to obtain cross relaxation and structural data.

Therefore, the conclusions of Edzes and Samulski that the protons of the bound water cross-relax with the protein protons (i.e., methyl proton group magnetic sinks), and that this effect is exhibited in the spin-lattice rather than the spin-spin relaxation data, appears to be correct. However, although these findings are in relatively good agreement with those from the previously presented ^3H NMR relaxation, it must be emphasized that the use of proton NMR complicates an already cumbersome problem. The appearance of a new cross relaxation term in the spin-relaxation data necessitates either additional NMR experiments or a creative use of different genetic variants of the same protein, as in the cited study.⁸ Clearly, the use of ^3H NMR or ^{17}O NMR relaxation experiments for proteins dissolved in D_2O , whereby cross relaxation is virtually eliminated in the T_1 process because of the large difference in the magnetic moments of these nuclei with protons, is much easier and more prone to success.

V. CONCLUDING REMARKS

The foregoing considerations add up to considerable agreement between certain theoretically and experimentally derived quantities. However, none of the above arguments should be interpreted as proof of any particular NMR mechanism or model, nor of the identity of the particular groups on the protein surface that interact with water. Even without such conclusions, and in place of the quest for absolute values of hydration, it can be useful to scrutinize relative changes in hydration when these can be taken as functions of changes in secondary, tertiary, or quaternary structure of a protein.

However, it must be stressed that the use of frequency-dependent NMR relaxation instruments in lieu of protein concentration-dependent relaxation measurements at a minimum of two

frequencies can yield erroneous results. High virial effects can indeed be present in protein solutions, especially if salt is not added to the system in order to minimize the protein-protein electrostatic potential. However, by use of nonlinear regression analysis, the virial coefficient of the protein, which is related to its net charge, can also be extracted from these protein concentration-dependent relaxation data.

Furthermore, although the NMR relaxation mechanism controversy still exists between the isotropic binding model and the intermediate asymmetry model, it can be concluded from all the above results that the "hydrodynamically influenced water" model of Koenig et al. can finally be placed to rest. Only a model whereby water directly binds to proteins can account for the water relaxation rate experiencing the charge of the macromolecule in protein solutions and for the protein structural results presented in this chapter. In addition, the model of water moving from site to site on the asymmetric surface of a macromolecule with a fast-motion component equal to the diffusion coefficient of unbound water, is also unlikely in protein solution. With the abundance of free water (i.e., 55.6 mol/l of water) relative to the protein concentration (approximately 10^{-3} mol/l), such a phenomenon would be thermodynamically unsound. On the other hand, in experiments involving protein powders and other two-phase biological systems, where only a limited amount of water is added to a solid or amorphous material and where surface adsorption of water to an insoluble second phase can exist, the above mechanism of asymmetric motion along the macromolecular surface most likely does predominate.

Therefore, in a true protein solution, only the isotropic two- or three-state binding mechanism or the water binding with a fast motional component to a macromolecule with a slow anisotropic motion are the most reasonable models of choice at this time.

One point with the above results should be noted here. The use of the ^1H NMR experiments which, of course, yield a sharp and well-defined water peak, can yield an extra relaxation resulting from fast-exchangeable protein protons, such as those arising from arginine, lysine, and even aspartic and glutamic acid side chains. However, in most cases, a calculation from the amino acid sequence of the protein in question can show the percentage contribution of this term to the results, and in most cases it will be small. Nevertheless, in the above studies, this effect would still not account for the change in hydration with temperature as observed for casein self-association, the β -lactoglobulin tetramerization, and the gelation of β -lactoglobulin at high pH. However, investigators may also perform the ^1H NMR relaxation experiments using ^{17}O NMR relaxation of the samples of protein dissolved in D_2O , if they are still plagued by the magnitude of this contribution to the hydration term.

Finally, the above absolute hydration results using a two- or three-state isotropic binding model are much lower than hydration values determined by small-angle X-ray scattering and sedimentation velocity experiments. It appears that only an asymmetric binding model could bring the order of magnitude in these hydration results in line with SAXS and hydrodynamic values. However, SAXS and hydrodynamic results may also contain another contribution not considered by some investigators. In fact, there may also be a dynamic contribution to the hydration, since it is measured by the difference between two volumes. The concept of protein "breathing" has been emphasized before,⁷¹ and the entire topic of protein dynamics has been reviewed recently.^{3,107} The effects of dynamic changes such as fluctuations (e.g., ring flipping and domain hinge bending) on packing volumes and accessible surface areas remain unclear. Progress on these questions may come from dynamic modeling by computer simulation.

ACKNOWLEDGMENT

The authors acknowledge a debt of gratitude to Norma C. Pessen for undertaking the demanding task of collating and checking the references, and for proofreading and correcting the successive versions of the entire manuscript.

1. Kuntz, I. D. and Kauzmann, W., Hydration of proteins and polypeptides. *Adv. Protein Chem.*, 28, 239, 1974.
2. Kumosinski, T. F. and Pessen, H., Estimation of sedimentation coefficients of globular proteins: an application of small-angle X-ray scattering. *Arch. Biochem. Biophys.*, 219, 89, 1982.
3. McCammon, J. A. and Karplus, M., The dynamic picture of protein structure. *Acc. Chem. Res.*, 16, 187, 1983.
4. Kumosinski, T. F. and Pessen, H., Structure and mechanism of action of riboflavin-binding protein: small-angle X-ray scattering, sedimentation, and circular dichroism studies on the holo- and apoproteins. *Arch. Biochem. Biophys.*, 214, 714, 1982.
5. Koenig, S. H. and Schillinger, W. E., Nuclear magnetic relaxation dispersion in protein solutions. *J. Biol. Chem.*, 244, 3283, 1968.
6. Koenig, S. H., Hallenga, K., and Shporer, M., Protein-water interaction studied by solvent ^1H , ^2H , and ^{13}C magnetic relaxation. *Proc. Natl. Acad. Sci. U.S.A.*, 72, 2667, 1975.
7. Halle, B., Andersson, T., Forsén, S., and Lindman, B., Protein hydration from water oxygen-17 magnetic relaxation. *J. Am. Chem. Soc.*, 103, 500, 1981.
8. Pessen, H., Purcell, J. M., and Farrell, H. M., Jr., Proton relaxation rates of water in dilute solutions of β -lactoglobulin. Determination of cross relaxation and correlation with structural changes by the use of two genetic variants of a self-associating globular protein. *Biochim. Biophys. Acta.* 828, 1, 1964.
9. Tanford, C., *Physical Chemistry of Macromolecules*. John Wiley & Sons, New York, 1961, 227, 293, 352, 563.
10. Schachman, H. K., *Ultracentrifugation in Biochemistry*. Academic Press, New York, 1959, 226.
11. Pedersen, K. O., Detailed theory. in *The Ultracentrifuge*. Svedberg, T. and Pedersen, K. O., Eds., Oxford University Press, London, 1940, 16.
12. Tiselius, A., Über den Einfluss der Ladung auf die Sedimentationsgeschwindigkeit von Kolloiden, besonders in der Ultrazentrifuge. *Kolloid-Z.*, 59, 306, 1932.
13. Booth, F., Sedimentation potential and velocity of solid spherical particles. *J. Chem. Phys.*, 22, 1956, 1954.
14. Pedersen, K. O., On charge and specific ion effects on sedimentation in the ultracentrifuge. *J. Phys. Chem.*, 62, 1282, 1958.
15. Timasheff, S. N. and Kronman, M. J., The extrapolation of light-scattering data to zero concentration. *Arch. Biochem. Biophys.*, 83, 60, 1959.
16. Kronman, M. J. and Timasheff, S. N., Light scattering investigation of ordering effects in silicotungstic acid solutions. *J. Phys. Chem.*, 63, 629, 1959.
17. Timasheff, S. N., The application of light scattering and small-angle X-ray scattering to interacting biological systems. in *Electromagnetic Scattering-I.C.E.S.*, Kerker, M., Ed., Pergamon Press/Macmillan, New York, 1963, 337.
18. Kirkwood, J. G. and Shumaker, J. B., Forces between protein molecules in solution arising from fluctuations in proton charge and configuration. *Proc. Natl. Acad. Sci. U.S.A.*, 38, 863, 1952.
19. Kirkwood, J. G. and Timasheff, S. N., The effect of ionization on the light scattering of isoionic proteins. *Arch. Biochem. Biophys.*, 65, 50, 1956.
20. Timasheff, S. N., Dintzis, H. M., Kirkwood, J. G., and Coleman, B. D., Light scattering investigation of charge fluctuations in isoionic serum albumin solutions. *J. Am. Chem. Soc.*, 79, 782, 1957.
21. Timasheff, S. N. and Tinoco, L., Light scattering of isoionic conalbumin. *Arch. Biochem. Biophys.*, 66, 427, 1957.
22. Timasheff, S. N. and Coleman, B. D., On light-scattering studies of isoionic proteins. *Arch. Biochem. Biophys.*, 63, 87, 1960.
23. Zimmerman, J. R. and Brittin, W. E., Nuclear magnetic resonance studies in multiple phase systems: lifetime of a water molecule in an adsorbing phase on silica gel. *J. Phys. Chem.*, 1328, 1957.
24. Hallenga, K. and Koenig, S. H., Protein rotational relaxation as studied by solvent ^1H and ^2H magnetic relaxation. *Biochemistry*, 15, 4255, 1976.
25. Lindstrom, T. R. and Koenig, S. H., Magnetic-field-dependent water proton spin-lattice relaxation rates of hemoglobin solutions and whole blood. *J. Magn. Reson.*, 15, 344, 1974.
26. Andree, P. J., The effect of cross relaxation on the longitudinal relaxation times of small ligands binding to macromolecules. *J. Magn. Reson.*, 29, 419, 1978.
27. Kumosinski, T. F. and Pessen, H., A deuterium and proton magnetic resonance relaxation study of β -lactoglobulin A association: some approaches to the Scatchard hydration of globular proteins. *Arch. Biochem. Biophys.*, 218, 286, 1982.
28. Casassa, E. F. and Eisenberg, H., Thermodynamic analysis of multicomponent solutions. *Adv. Protein Chem.*, 19, 287, 1964.
29. Na, G. C. and Timasheff, S. N., Interaction of calf brain tubulin with glycerol. *J. Mol. Biol.*, 151, 165, 1981.
30. Tanford, C., Extension of the theory of linked functions to incorporate the effects of protein hydration. *J. Mol. Biol.*, 39, 539, 1969.

31. Kubo, R. and Tomita, K., A general theory of magnetic resonance absorption. *J. Phys. Soc. Jpn.*, 9, 888, 1954.
32. Solomon, I., Relaxation processes in a system of two spins, *Physiol. Rev.*, 99, 559, 1955.
33. Abragam, A., *The Principles of Nuclear Magnetism*. Oxford University Press (Clarendon), London, 1961. chap. 8.
34. Walmsley, R. H. and Shporer, M., Surface-induced NMR line splittings and augmented relaxation rates in water. *J. Chem. Phys.*, 68, 2584, 1978.
35. Berendsen, H. J. C. and Edzes, H. T., The observation and general interpretation of sodium magnetic resonance in biological material. *Annu. N.Y. Acad. Sci.*, 204, 459, 1973.
36. Edzes, H. T. and Samulski, E. T., The measurement of cross relaxation effects in the proton NMR spin-lattice relaxation of water in biological systems: hydrated collagen and muscle. *J. Magn. Reson.*, 31, 207, 1978.
37. Townend, R., Winterbottom, R. J., and Timasheff, S. N., Molecular interactions in β -lactoglobulin. II. Ultracentrifugal and electrophoretic studies of the association of β -lactoglobulin below its isoelectric point. *J. Am. Chem. Soc.*, 82, 3161, 1960.
38. Vold, R. L., Waugh, J. S., Klein, M. P., and Phelps, D. E., Measurement of spin relaxation in complex systems. *J. Chem. Phys.*, 48, 3831, 1968.
39. Bloch, F., Nuclear induction. *Physiol. Rev.*, 70, 460, 1946.
40. Gerhards, R. and Dietrich, W., The analysis of spin-lattice relaxation time experiments. *J. Magn. Reson.*, 23, 21, 1976.
41. Sass, M. and Ziessow, D., Error analysis for optimized inversion recovery spin-lattice relaxation measurements. *J. Magn. Reson.*, 25, 263, 1977.
42. Kowalewski, J., Levy, G. C., Johnson, L. F., and Palmer, L., A three-parameter non-linear procedure for fitting inversion-recovery measurements of spin-lattice relaxation times. *J. Magn. Reson.*, 26, 533, 1977.
43. Brunetti, A., Computation of T_1 from pulsed NMR data using a generalized and rapid least-squares formula. *J. Magn. Reson.*, 28, 289, 1977.
44. Leipert, T. K. and Marquardt, D. W., Statistical analysis of NMR spin-lattice relaxation times. *J. Magn. Reson.*, 24, 181, 1976.
45. Becker, E. D., Ferretti, G. A., Gupta, R. K., and Weiss, G. H., The choice of optimal parameters for measurement of spin-lattice relaxation times. II. Comparison of saturation recovery, inversion recovery, and fast inversion recovery experiments. *J. Magn. Reson.*, 37, 381, 1980.
46. Farrar, T. C. and Becker, E. D., *Pulse and Fourier Transform NMR: Introduction to Theory and Methods*. Academic Press, New York, 1971, 92.
47. Timasheff, S. N. and Townend, R., Molecular interactions in β -lactoglobulin. VI. The dissociation of the genetic species of β -lactoglobulin at acid pH's. *J. Am. Chem. Soc.*, 83, 470, 1961.
48. Witz, J., Timasheff, S. N., and Luzzati, V., Molecular interactions in β -lactoglobulin. VIII. Small-angle X-ray scattering investigation of the geometry of β -lactoglobulin A tetramerization. *J. Am. Chem. Soc.*, 86, 168, 1964.
49. Townend, R. and Timasheff, S. N., Molecular interactions in β -lactoglobulin. III. Light scattering investigation of the stoichiometry of the association between pH 3.7 and 5.2. *J. Am. Chem. Soc.*, 82, 3168, 1960.
50. Kumosinski, T. F. and Timasheff, S. N., Molecular interactions in β -lactoglobulin. X. The stoichiometry of the β -lactoglobulin mixed tetramerization. *J. Am. Chem. Soc.*, 88, 5635, 1966.
51. Timasheff, S. N. and Townend, R., Molecular interactions in β -lactoglobulin. V. The association of the genetic species of β -lactoglobulin below the isoelectric point. *J. Am. Chem. Soc.*, 83, 464, 1961.
52. Timasheff, S. N. and Townend, R., β -lactoglobulin as a model of subunit enzymes. *Protides Biol. Fluids*, 16, 33, 1969.
53. Kalk, A. and Berendsen, H. J. C., Proton magnetic relaxation and spin diffusion in proteins. *J. Magn. Reson.*, 24, 343, 1976.
54. Koenig, S. H., Bryant, R. G., Hallenga, K., and Jacob, G. S., Magnetic cross relaxation among protons in protein solutions. *Biochemistry*, 17, 4348, 1978.
55. Kumosinski, T. F., Pessen, H., and Purcell, J. M., Use of proton NMR relaxation rates in the determination of the thermodynamics of primary hydration in an associating protein system (β -lactoglobulin). *Fed. Proc. Fed. Am. Soc. Exp. Biol.*, 39, 1673, 1980.
56. Timasheff, S. N. and Townend, R., Molecular interactions in β -lactoglobulin. I. The electrophoretic heterogeneity of β -lactoglobulin close to its isoelectric point. *J. Am. Chem. Soc.*, 82, 3157, 1960.
57. Waldstein, P., Rabideau, S. W., and Jackson, J. A., Nuclear magnetic resonance of single crystals of D_2O ice. *J. Chem. Phys.*, 41, 3407, 1964.
58. Timasheff, S. N. and Townend, R., Structure of the β -lactoglobulin tetramer. *Nature*, 203, 517, 1964.
59. Hunt, M. J. and Mackay, A. L., Deuterium and nitrogen pure quadrupole resonance in deuterated amino acids. *J. Magn. Reson.*, 15, 402, 1974.
60. Poole, C. P. and Farach, H. A., *Relaxation in Magnetic Resonance*. Academic Press, New York, 1971, 65.
61. Pessen, H., Kumosinski, T. F., and Timasheff, S. N., Small-angle X-ray scattering. *Methods Enzymol.*, 27, 151, 1973.

62. Wahl, P. and Timasheff, S. N., Polarized fluorescence decay curves for β -lactoglobulin A in various states of association. *Biochemistry*, 8, 2945, 1969.
63. Ceccarelli, C., Jeffrey, G. A., and Taylor, R., A survey of O-H...O hydrogen bond geometries determined by neutron diffraction. *J. Mol. Struct.*, 70, 255, 1981.
64. Wyman, J., Jr., Linked functions and reciprocal effects in hemoglobin: a second look. *Adv. Protein Chem.*, 19, 223, 1964.
65. Gilbert, G. A., General discussion on the physical chemistry of enzymes. Characterization and physical properties. *Discuss. Faraday Soc.*, 20, 68, 1955.
66. Gilbert, G. A., Sedimentation and electrophoresis of interacting substances. I. Idealized boundary shape for a single substance aggregating reversibly. *Proc. R. Soc. London, Ser. A*, 250, 377, 1959.
67. Cooke, R. and Kuntz, I. D., The properties of water in biological systems. *Annu. Rev. Biophys. Bioeng.*, 3, 95, 1974.
68. Hagler, A. T. and Moulton, J., Computer simulation of the solvent structure around biological macromolecules. *Nature*, 272, 222, 1978.
69. Teller, D., Swanson, E., and De Haen, C., The translational friction coefficient of proteins. *Methods Enzymol.*, 61, 103, 1979.
70. Whitney, R. McL., Brunner, J. R., Ebner, K. E., Farrell, H. M., Jr., Josephson, R. V., Morr, C. V., and Swaisgood, H. E., Nomenclature of the proteins of cow's milk: fourth revision. *J. Dairy Sci.*, 59, 785, 1976.
71. Brown, E. M. and Pfeffer, P. E., Relative exposure of lysine groups in β -lactoglobulin. *Fed. Proc. Fed. Am. Soc. Exp. Biol.*, 40, 1615, 1981.
72. Schoenborn, B. P. and Hanson, J. C., The determination of structural water by neutron protein crystallography: an analysis of the carbon monoxide myoglobin water structure. in *Water in Polymers*. Rowland, S. P., Ed., American Chemical Society, Washington, D.C., 1980, 217.
73. Farrell, H. M., Jr. and Thompson, M. P., The caseins as calcium binding proteins. in *Calcium Binding Proteins*. Thompson, M. P., Ed., CRC Press, Boca Raton, FL, 1986.
74. Eigel, W. N., Butler, J. E., Ernstrom, C. A., Farrell, H. M., Jr., Harwalkar, V. R., Jenness, R., and Whitney, R. McL., Nomenclature of proteins of cow's milk: fifth revision. *J. Dairy Sci.*, 67, 1599, 1984.
75. Slattery, C. W. and Evard, R., A model for the formation and structure of casein micelles from subunits of variable composition. *Biochim. Biophys. Acta*, 313, 529, 1973.
76. Pepper, L. and Farrell, H. M., Jr., Interactions leading to formation of casein submicelles. *J. Dairy Sci.*, 65, 2259, 1982.
77. Schmidt, D. G., Association of caseins and casein micelle structure in *Developments in Dairy Chemistry*, Vol. 1, Fox, P. E., Ed., Applied Science, Essex, England, 1982.
78. Kumosinski, T. F., Pessen, H., Prestrelski, S. J., and Farrell, H. M., Jr., Water interactions with varying molecular states of bovine casein: ^2H NMR relaxation studies. *Arch. Biochem. Biophys.*, 257, 259, 1987.
79. Davies, D. T. and Law, A. J. R., Content and composition of protein in creamery milks in South-West Scotland. *J. Dairy Res.*, 47, 83, 1980.
80. Carroll, R. J. and Farrell, H. M., Jr., Kappa-casein: an immunological approach to its location in the casein micelle using electron microscopy. *J. Dairy Sci.*, 66, 679, 1983.
81. Pessen, H. and Kumosinski, T. F., Measurements of protein hydration by various techniques. *Methods Enzymol.*, 117, 219, 1985.
82. Capalja, G. G., An electron microscope study of the ultrastructure of bovine and human casein micelles in fresh and acidified milk. *J. Dairy Res.*, 35, 1, 1968.
83. Schultz, B. C. and Bloomfield, V. A., Structure of bovine casein oligomers. *Arch. Biochem. Biophys.*, 173, 18, 1976.
84. Clarke, R. and Nakai, S., Investigation of κ - α_1 -casein interaction by fluorescence polarization. *Biochemistry*, 10, 3353, 1971.
85. Pepper, L., Casein interactions as studied by gel chromatography and ultracentrifugation. *Biochim. Biophys. Acta*, 278, 147, 1972.
86. Tanford, C., *Physical Chemistry of Macromolecules*. John Wiley & Sons, New York, 1961, 236.
87. Arakawa, T. and Timasheff, S. N., Preferential interactions of proteins with salts in concentrated solutions. *Biochemistry*, 21, 6545, 1982.
88. Timasheff, S. N. and Townend, R., Structural and genetic implications of the physical and chemical differences between β -lactoglobulins A and B. *J. Dairy Sci.*, 45, 259, 1962.
89. Timasheff, S. N., The nature of interactions in proteins derived from milk. in *Symposium on Foods: Proteins and Their Reactions*. Schultz, H. W. and Angelmeier, A. F., Eds., AVI Publishing, Westport, CT, 1964, 174.
90. Townend, R., β -lactoglobulins A and B: the environment of the Asp/Gly difference residue. *Arch. Biochem. Biophys.*, 109, 1, 1965.
91. Waissbluth, M. D. and Grieger, R. A., Alkaline denaturation of β -lactoglobulins. Activation parameters and effect on dye binding site. *Biochemistry*, 13, 1285, 1974.

92. Grösch, L. and Noack, F., NMR relaxation investigation of water mobility in aqueous bovine serum albumin solutions. *Biochim. Biophys. Acta.* 453, 218, 1976.
93. Aschaffenburg, R. and Drewry, J., Occurrence of different β -lactoglobulins in cow's milk. *Nature.* 176, 218, 1955.
94. Cooke, R. and Kuntz, I. D., The properties of water in biological systems. *Annu. Rev. Biophys. Bioeng.* 3, 95, 1974.
95. Green, D. W., Aschaffenburg, R., Camerman, A., Coppola, J. C., Dunnill, P., Simmons, R. M., Komorowski, E. S., Sawyer, L., Turner, E. M. C., and Woods, K. F., Structure of bovine β -lactoglobulin at 6Å resolution. *Mol. Biol.* 131, 375, 1979
96. Dayhoff, M. O., Ed., *Atlas of Protein Sequence and Structure*. Vol. 5. Suppl. 1, National Biomedical Research Foundation. Washington, D.C., 1973. S-83.
97. Townend, R., Weinberger, L., and Timasheff, S. N., Molecular interactions in β -lactoglobulin. IV. The dissociation of β -lactoglobulin below pH 3.5. *J. Am. Chem. Soc.* 82, 3175, 1960.
98. Georges, C., Guinand, S., and Tonnelat, J., Etude thermodynamique de la dissociation réversible de la β -lactoglobuline B pour des pH supérieurs à 5.5. *Biochim. Biophys. Acta.* 59, 737, 1962.
99. McKenzie, H. A. and Sawyer, W. H., Effect of pH on β -lactoglobulins. *Nature.* 214, 1101, 1967.
100. Roels, H., Préaux, G., and Lontie, R., Polarimetric and chromatographic investigation of the irreversible transformation of β -lactoglobulin A and B upon alkaline denaturation. *Biochimie.* 53, 1085, 1971.
101. Brown, E. M. and Farrell, H. M., Jr., Interaction of β -lactoglobulin and cytochrome c: complex formation and iron reduction. *Arch. Biochem. Biophys.* 185, 156, 1978.
102. Oncley, G. L., The electric moments and the relaxation times of proteins as measured from their influence upon the dielectric constants of solutions. in *Proteins, Amino Acids, and Peptides*. Cohn, E. J. and Edsall, J. T., Eds., Reinhold, New York, 1943, 557, 563.
103. Shirley, W. M. and Bryant, R. G., Proton-nuclear spin relaxation and molecular dynamics in the lysozyme-water system. *J. Am. Chem. Soc.* 104, 2910, 1982.
104. Daskiewicz, O. K., Hennel, J. W., Lubas, B., and Szczepkowski, T. W., Proton magnetic relaxation and protein hydration. *Nature.* 200, 1006, 1963.
105. Beall, P. T., Hazlewood, C. F., and Rao, P. N., Nuclear magnetic resonance patterns of intracellular water as function of HeLa cell cycle. *Science.* 192, 904, 1976.
106. Lee, J. C. and Timasheff, S. N., Partial specific volumes and interactions with solvent components of proteins in guanidine hydrochloride. *Biochemistry.* 13, 257, 1974.
107. Petsko, A. and Ringe, D., Fluctuations in protein structure from X-ray diffraction. *Annu. Rev. Biophys. Bioeng.* 13, 331, 1984.
108. Tanford, C., Bunville, L. G., and Nozaki, Y., The reversible transformation of β -lactoglobulin at pH 7.5. *J. Am. Chem. Soc.* 81, 4032, 1959.